Analysis of Peristaltic Eyring-Powell Fluid with an Inclined Magnetic Field in a non-Uniform Porous Channel

BY
SARA JABEEN

NATIONAL UNIVERSITY OF MODERN LANGUAGES
ISLAMABAD
AUGUST 2024

Analysis of Peristaltic Eyring-Powell Fluid with an Inclined Magnetic Field in a non-Uniform Porous Channel

BY
SARA JABEEN

MS MATH, NATIONAL UNIVERSTY OF MODERN LANGUAGES ISALMABAD 2024

A THESIS SUBMITTED IN PARTIAL FULFILMENT OF
THE REQUIREMENTS FOR THE DEGREE OF

MASTER OF SCIENCE

In **MATHEMATICS**

TO

FACULTY OF ENGINEERING AND COMPUTING

NATIONAL UNIVERSITY OF MODERN LANGUAGES ISLAMABD
© Sara Jabeen 2024

NATIONAL UNIUVERSITY OF MODERN LANGUAGES   FACULTY OF ENGINEEIING & COMPUTER SCIENCE

THESIS AND DEFENSE APPROVAL FORM

The undersigned certify that they have read the following thesis, examined the defense, are satisfied with overall exam performance, and recommend the thesis to the Faculty of Engineering and Computing for acceptance.

Thesis Title: Analysis of Peristaltic Eyring-Powell Fluid with an Inclined Magnetic Field in a non-Uniform Porous Channel

Submitted By: Sara Jabeen   **Registration #:** 66 MS/MATH/F22

Master of Science in Mathematics (MS Math)
Title of the Degree

Mathematics
Name of Discipline

Dr. Hadia Tariq
Name of Research Supervisor   Signature of Research Supervisor

Dr. Sadia Riaz
Name of HOD (Math)   Signature of HOD (Math)

Dr. Noman Malik
Name of Dean (FEC)   Signature of Dean (FEC)

Date: 6th August, 2024

AUTHOR'S DECLARATION

I <u>Sara Jabeen</u>

Daughter of <u>Nasir Ali</u>

Registration # <u>66 MS/Math/F22</u>

Discipline <u>Mathematics</u>

Candidate of **Master of Science in Mathematics (MS MATH)** at the National University of Modern Languages do hereby declare that the thesis **Analysis of Peristaltic Eyring-Powell fluid with Inclined Magnetic Field in a Non-Uniform Porous Channel** submitted by me in partial fulfillment of MS Math degree, is my original work, and has not been submitted or published earlier. I also solemnly declare that it shall not, in future, be submitted by me for obtaining any other degree from this or any other university or institution. I also understand that if evidence of plagiarism is found in my thesis/dissertation at any stage, even after the award of a degree, the work may be cancelled and the degree revoked.

Signature of Candidate

Sara Jabeen

Name of Candidate

6th August, 2024

Date

ABSTRACT

Title: Analysis of Peristaltic Eyring-Powell Fluid with an Inclined Magnetic Field in a Non-Uniform Porous Channel

The main focus of this thesis is to investigate the peristaltic transport of an Eyring-Powell fluid in a non-Uniform porous channel under an inclined magnetic field. The study also takes into consideration wall properties. The governing equations for the conservation of mass and momentum for Eyring-Powell fluid in a symmetric channel are introduced. Stream functions are used to reduce the number of dependent variables of governing PDEs. Perturbation method is used to solve these equations in order to obtain velocity and temperature profiles. The effects of diverse parameter on streamlines, velocity, pressure and temperature are investigated. The software Mathematica is used to create the graphs.

TABLE OF CONTENTS

LIST OF FIGURES

LIST OF SYMBOLS

A, B	Material Derivatives
ρ	Density
p	Pressure
μ	Viscosity
a	Width
b	Amplitude
c	Wave Speed
λ	Wavelength
β_0	Applied Magnetic Field
n	Dimensional parameter
ψ, φ	Stream Function
E_1, E_2, E_3	Wall Properties
u	Velocity of Fluid in x Direction
v	Velocity of fluid in y Direction
Re	Reynold Number
α	Inclination of the Channel
Ec	Eckert Number
k	Porosity parameter
δ	Wave Number

ACKNOWLEDGMENT

DEDICATION

This thesis is dedicated to my parents, and my teachers who always supported and taught me to work hard for the things that I aspire to achieve. All of them have been a source of motivation and strength during moments of despair and discouragement

CHAPTER 1

INTRODUCTION AND LITERATURE REVIEW

1.1   Introduction

The study of fluid motion and the forces acting on it is the focus of fluid mechanics. Like all mathematical representations of the real world, fluid mechanics is predicated on a few basic beliefs about the materials being studied. Interestingly, the concepts of fluid mechanics are not limited to ordinary liquids and gases; they also apply to a wider variety of materials. If fluids can be thought of as continuous media, then this field aims to characterize macroscopic fluid flow and related phenomena. This presumption means that any fluid component with a tiny volume is large enough to hold a significant number of molecules.

1.2   Peristalsis

In fluid mechanics, peristalsis can be defined as the self-propagation motion of fluids that relies on the wave-like action of contraction and relaxation. Peristalsis is of utmost importance in multiple domains of life prominently in the functioning of the human body and specific technological applications. Peristaltic mechanism found in digestive systems, blood circulation, artificial muscles, insect locomotion, environmental monitoring and pharmaceutical manufacturing. The mechanism of peristalsis was mathematically presented by Latham [1] who has investigated the theoretical and experimental results of the movement of urine through the ureter by using Newtonian compressible fluids. Peristalsis is mostly studied in non-Newtonian fluids because of its wave-like motion and gradual changes in viscosity and shear stress can

handle these fluids in a more delicate manner.

Later, Shapiro *et al*. [2] conducted research on the mechanism of peristalsis in situations involving long wavelengths and low Reynolds numbers. Researchers use these conditions because low Reynolds numbers represent that inertial effects in flow are negligible and long wavelengths tell us pressure to be considered uniform. Rani and Sarojamma [3] investigated the peristaltic Casson fluid transport in a two-dimensional asymmetric channel. It also looked at the occurrences of reflux and entrapment in symmetric channels, with a particular emphasis on low Reynolds number and long-wavelength situations. The work of Burns and Parkes [4] involved peristaltic motion in two-dimensional and axisymmetric cases, adopting low Reynolds numbers and linearized boundary conditions. Bhatti *et al*. [5] discussed how peristaltic blood circulation of Ree-Eyring fluid and wall characteristics were affected by the incorporated effects of hydrodynamic magnetization and partial sliding. Sucharita *et al*. [6] investigated the analytical approaches for peristaltic movement and heat exchange of a Herschel-Bulkley fluid in a sloped non-uniform duct with wall properties.

Rajashekar *et al*. [7] analyzed the behavior of blood flow in two layers employing the Herschel-Bulkley fluid in an axisymmetric tube. They assessed the outcomes using long wavelength measurements and low Reynold numbers assumptions. The study identifies differences in flux, dynamics of frictional forces and increase in pressure. It was noticed that the Herschel-Bulkley model exhibits dissimilar behavior as comparison to alternative Newtonian and Power-Law models. Mansour and Abou-Zeid [8] investigated the impact of mass and heat transmission on Williamson fluid's peristaltic flow in the irregular vertical tube. The temperature rised as the Eckert number (Ec) and Weissenberg number (We) grew, while the concentration follows an opposite trend. Additionally, axial velocity decreased with the rising Eckert number, Gasthof number, and modified Grasthof number while it increases with increasing Schmidt number (Sc) and Sherwood number (Sr). Baligha *et al.* [9] examined how Herschel-Bulkley fluid flow in a tube was affected by temperature and velocity slip. They discovered that frictional forces behave differently with temperature and that the pressure rise in a fluid under peristaltic forcing higher than in a fluid. Puranik *et al*. [10] analyzed the effects of a Newtonian fluid in peristaltic

flow through impermeable eccentric cylinders by using perturbation technique. They found that as the Grashof number rises, velocity, pressure gradient and temperature also rise in eccentric cylinders relative to concentric ones.

1.3   Eyring-Powell Fluid Model

Eyring and Powell created the Eyring-Powell fluid model in 1944. The behavior of fluid flows in the endoscope was studied by Akbar *et al*. [11] to understand the levels of shear stress and interaction with heating mechanisms. Although the model of Eyring-Powell fluid is mathematically an intricate model, however, it is favored above alternative non-Newtonian models primarily for two reasons. Firstly, this model is created using the liquids kinetic theory except from the power law model which is used in non-Newtonian fluids. Secondly, this model illustrates the nature of both Newtonian and non-Newtonian fluids for low and high shear rates.

This model can be utilized in certain circumstances to explain the viscoelastic behavior of polymer solutions, viscous suspension across a broad range of shear rates, molecular diffusion, and lubrication technology. Modeling peristaltic transport in a variety of applications requires the use of Eyring-Powell fluids, which exhibit shear-thinning behavior and are non-Newtonian fluids. Their excellent representation of the rheological characteristics of fluids subjected to peristaltic motion enhances biological and medical device predictions. This is crucial for the administration of medications, gastrointestinal functions, and prosthetic organs. Eyring-Powell fluid models help us better explained and conduct peristaltic transport overall. This model helps in understanding the fluid dynamics included in food propulsion through the digestive system, contributing to better insights into nutrient absorption and digestion. Qasim and Noreen [12] had examined the peristaltic transport of incompressible magneto hydrodynamic Eyring-Powell fluid in the planar channel. Khan *et al*. [13] looked at the way entropy formation influences a steady, non-Newtonian Eyring-Powell fluid in two dimensions in a permeable channel by employing homotopy analysis and shooting technique. It was noticed that the Bejan number had a minimum value at the top plate and a maximum value at the middle of the channel, and that the Eyring-Powell fluid characteristics limit the flow.

Ahmad *et al*. [14] created a mathematical model for the Peristaltic Powell-Eyring nanomaterial and studied the transfer of mass and heat with a magnetic field. Applications of this paradigm include enzymatics, thermal technology, medicinal research, and cancer therapy. Iqbal *et al*. [15] analyzed the effect of various factors on viscosity properties and peristaltic flow of Powell-Eyring nanofluid. The outcome revealed that changes in fluid properties, heat sources, and sinks increase heat transmission rates, concentration dispersion, and mass transfer rates. Bhattacharyya *et al*. [16] examined mass transfer and heat characteristics of the Eyring-Powell fluid's peristaltic transit in a uniform or non-uniform conduit while taking Joule heating and wall flexibility into account. M.Gudekote *et al*. [17] investigated the peristaltic flow properties of an Eyring Powell fluid through a non-uniform channel. Variable viscosity, variable heat conductivity, and slip were all taken into account in the research. Akbar *et al*. [18] discussed the thermodynamical analysis for dynamic Powell Eyring magneto nanofluid enhanced peristaltic movement with mass transfer in electroosmosis. The electro-kinetic pumping phenomena when combined with the peristaltic phenomenon enhances the efficiency of smart pumps for medical and nanotechnology applications.

Nadeem *et al*. [19] included Al_2O_3 for the porosity (*V*) parameter and studied the non-Newtonian viscoelastic Eyring Powell Nanofluid's mathematical behavior. M.Boujelbene *et al*. [20] investigated the transport of Eyring-Powell fluid peristaltically over a uniform conduit. The study was carried out with wall characteristics present and varied liquid properties. Akram *et al*. [21] examined that in an asymmetric channel with magnetic flux, partial slip influnces Eyring-Powell nanofluid double diffusion convection on peristaltic flow. Choudhari *et al*. [22] used a non-Newtonian third-grade fluid to model the peristalsis process while taking into account the fluid's properties, electroosmosis, slip, and chemical interactions. It looked at how variations affect concentration, temperature, velocity, and trapping. Yasin *et al*. [23] investigated the strong force fields while examining the effects of Slip and Hall current on MHD Eyring-Powell fluid transfer.

1.4   Porous medium

Materials that are porous, such as rocks or sponges, are full of microscopic voids. Water, air, and other materials can be contained in these areas. Filters and several other processes depend on them, as does groundwater flow. The analysis of fluid mechanics by using porous media is of significant importance in different technological fields including biological applications. Porous mediums are used in fluid mechanics due to their ability to change the behavior of fluid flows in different ways. It can enhance heat and mass transfer, reduce drag in fluid flow, used for filtration and separation processes.

Darcy [24] defined the flow rate in the porous material. He looked at the resistance factor caused by the porous medium's permeability experimentally. Funmilay and Moses [25] investigated heat exchange by naturally occurring convection on an unstable magneto hydrodynamic stream of non-Newtonian fluids using a porous channel. Nazeer *et al*.[26] analyzed the thermal transportation of the Jeffrey fluid in a porous media with pliable walls and discovered that radiation modifies temperature profiles and lowers fluid velocity by adding thermal energy. M. Eldesoky *et al*. [27] examined the viscous Maxwell fluid's peristaltic motion in a porous media and found that reverse flow and net flow rate were highly influenced by physical characteristics. Javed *et al*. [28] examined how biological fluid flow in curved channels was affected by porosity. They discovered that sinusoidal waves boost porosity effects, increasing effectiveness and opening up new bioengineering possibilities for chemical processes and medication delivery systems. Noreen *et al*. [29] looked at how an inclined magnetic field affected the heat transfer behavior of Carreau fluids in an inclined asymmetric channel. It approximates solutions to complex problems by using perturbation techniques. The study reveals temperature properties and velocity distribution control, which was useful in the design of peristaltic pumps for non-Newtonian physiological liquids.

Ahmed *et al*. [30] analyzed the characteristics of heat and mass transport in an asymmetric porous channel while a nanofluid is peristaltically flowing with the effect of magnetic and adding temperature-dependent viscosity. Vijayaragawan *et al*. [31] examined the peristaltic motion of a Jeffrey fluid in a permeable medium while taking into account the fluid's graphical

representations, velocity slip parameters, and an external magnetic field. Jagadesh *et al*. [32] studied free convective peristaltic pumping of a Casson fluid. This study reveals that increasing Casson and magnetic parameters enhances heat transfer rate and streamlines.

1.5   Magnetic Hydrodynamics

In the domain of fluid mechanics, MHD investigates the dynamics of liquid metals, ionized gases and electrically conducting fluids under the influence of magnetic fields. The interaction of magnetic field with electrically conducting fluids create a vast domain for investigation and inventive advancements. Researchers use MHD to examine the diverse array of phenomena with applications extending from biomedical applications to space exploration. Applications for magnetohydrodynamic flows are many and include cancer therapy, materials processing, biomedical flow control, MHD energy generators, MHD drug targeting, magnetofluid rotary blood pumping, and separation devices. Devakar *et al*. [33] analyzed the effects of magneto hydrodynamics on peristaltic movement of couple stress fluid by using two concentric inclined channels, one in endoscope and other has traveling down its wall. It was observed that the magnetic push opposes the flow, and the peristaltic flow's pumping rate increases as the tube moves from horizontal to vertical. Khan and Rafaqat [34] explored the peristaltic flow caused by surface acoustic waves and its implications in geophysics and the aircraft industry, using magnetohydrodynamics (MHD) and heat transfer in compressible fluids.

Nabil T. M. El-Dabe *et al*. [35] examined the heat radiation and Ohmic dissipation effects of the MHD cyclical flow of a stable, incompressible power-law nanofluid in a non-Darcy porous medium.Rafiq *et al*. [36] discussed the activation energy's impact, variable characteristics and magneto hydrodynamics on the Jeffery fluid's peristaltic flow using porous wall channel. The study offered that the current analysis may be applied to investigate numerous human physiological systems specifically, the blood flow. Abd-Alla *et al.* [37] examined the impact of heat and mass transfer on the magneto hydrodynamic Jeffery nanofluid's peristaltic flow through

inclined symmetric channels with porous media. Hayat *et al.* [38] looked at the MHD hybrid nanomaterial's peristaltic movement in an asymmetric porous channel. Convection, radiation, dissipation, and Hall current were all taken into account when building the analysis. Hafez *et al*. [39] explored how heat and mass transfer affect a Casson fluid's hydro-magnetic peristaltic flow in a system that was inclined and rotated. Mathematica software was used in the study to examine numerical findings and equations. The findings indicate that while the permeability parameter increased the confined bolus size, velocity slip reduces it.

Tanveer *et al*. [40] examined the entropy generation phenomena that results from a peristaltic process on a curved surface. In this study, the effects of changing viscosity, convective circumstances, and MHD on the governing system of equations was used. Hussein and T.Eldabe [41] investigated the peristaltic flow under the effect of variable electrical conductivity along a vertical asymmetric channel equipped with a third order magnetic nanofluid model immersed in a permiable material. J. Iqbal and F. M. Abassi [42] investigated the features of magnetohydrodynamics (MHD) peristaltic transport by taking into account the characteristics of aluminum and zinc oxide nanoparticles floating in water via an asymmetrically bent conduit. Magesh *et al*. [43] used asymmetric channels, magnetic fields, gravity, and graphical representations to study the peristaltic transport of an Oldroyd-B fluid in an inclined channel.

Tanveer and Jarral [44] looked at the effects of inclined magnetohydrodynamics (MHD) with slip boundary conditions in a tapered asymmetric porous channel with peristalsis. It displayed physical properties and generates numerical solutions using Mathematica software. In peristaltic flow for non-Newtonian Jeffrey fluid, the research emphasized the interaction of Joule heating, Darcy resistance, and tilted magnetic field effects. Y.Elmhedy *et al*. [45] looked at the impact of magnetic fields and heat transfer in peristaltic flow of a model of a Rabinowitsch fluid in an inclined channel. It used an incompressible Rabinowitsch fluid to study peristalsis with heat transmission when a magnetic field is present. Computational simulations were used in the study to examine flow rates as well as the effects of magnetic field and heat transfer factors.

1.6   Non-Uniform Channel

In the context of fluid dynamics, a non-uniform channel defines a conduit through which fluid flows, showcasing changes in shape, area and other features along its length. This variation in geometry tells the difference between non-uniform and uniform channels, where cross sectional properties remain unchanged. In Biological systems, Peristaltic motion is a common way of fluid conveyance. The geometry of these systems is mostly non-uniform, providing researchers better means to replicating fluid behavior within a biological framework. Akram *et al*. [46] analyzed the impacts of warmth and concentrated fluctuation on the non-uniform inclined channel peristaltic transport of nanofluids.R Shukla *et al.* [47] examined the influence of the roughness parameter on a Newtonian fluid's peristaltic movement in an irregular channel with a sinusoidal shape has been investigated. The flexible characteristics of the liquid, analytical findings for the unstable motion of a Rabinowitsch fluid were derived by C Rajashekhar *et al.* [48].

It is believed that the Rabinowitsch fluid flows via an inclined, non-uniform channel and originates in both homogeneous and heterogeneous chemical processes.Khan *et al*. [49] investigated how Double diffusive convection and an angled magnetic field in nanofluids influence the peristaltic pumping of fourth-grade fluid in non-uniform channels. It was observed that increased thermophoresis effects decreased fluid viscosity, lowering the percentage of less dense nanoparticles, but elevated Brownian motion increased nanoparticle density and therefore the nanoparticle fraction.

Ibrahim and Abou-zeid [50] examined the mixed convection magnet Nano's flow mechanism in Prandtl fluid, offering information for the use of drug-carrying systems in hypoxic tumor environments. Manjunatha *et al*. [51] analyzed how the Jeffery fluid's flow in a non-uniform conduit was affected by mass and heat transfer. Concentration profiles enhanced the confined bolus volume, but variable viscosity raised the temperature, velocity, and Nusselt number fields.

1.7   Contribution to thesis

A thorough analysis of Hina's work is included in this thesis. It investigates the effects of the partial slip, wall characteristics, and magnetic field on the Eyring-Powell fluid's peristaltic flow. Important influences of viscous dissipation are investigated in the formulation in mathematics. With the long wavelength and low Reynolds number conditions met, a perturbation solution is obtained. The computational study was performed using Mathematica software, and the findings will be shown graphically.

1.8   Thesis Organization

The material below provides a clear overview of the thesis' contents.

Chapter 2 presents basic concepts and dimensionless parameters that are utilized to obtain numerical results for the flow problem.

Chapter 3 provides the review of work done by Hina [55] which gives thorough analysis of the heat transmission, slip conditions, and wall properties associated with MHD peristaltic flow of Eyring-Powell fluid.

Chapter 4 extends the review work by considering the impact of inclined magnetic field on the Eyring-Powell fluid peristaltic motion in a non-uniform permeable medium.

Chapter 5 concludes by discussing the overall study project and the potential applications of the findings for future work.

In the end, all the references utilized in this research are listed.

CHAPTER 2

Basic Definitions and Concepts

Basic definitions and instructions are provided in this chapter to aid readers in understanding the analysis.

2.1 Fluid mechanics

The study of mechanics is concerned with the influence of forces on bodies which we experience in both nature and technology. It has been divided into statics and dynamics. Stationary bodies fall under the category of statics whereas bodies in motion are concerned with dynamics. The study of the effects of forces on fluids (at rest as well as in motion) is known as Fluid Mechanics. In multiple domains of life, fluid mechanics plays a significant role in fostering progress and maximizing efficiency.

It has been applied in such areas as designing vehicles, predicting weather patterns, developing flow measurement devices, the aerodynamics of large buildings, and understanding the behavior of biological fluids such as blood, air or synovial fluid. There are two methods to study fluid mechanics: Macroscopic and microscopic methods.

In the microscopic approach, we study the behavior of fluids on the molecular level while in the macroscopic approach, we study the average behavior of fluids. Mostly, Fluid mechanics is supposed to describe at the macroscopic level, [52].

2.2 Fluid

In simple words, Fluid can be defined as "any substance which can flow". A precise definition of a fluid is that it is a substance that undergoes continuous deformation irrespective of how negligible shear stress may be. Two categories of fluids exist. Liquids have a constant volume and are made up of molecules that are packed relatively closely together with strong cohesive forces. In contrast, the molecules in gases are widely separated, have no defined volume, and very little cohesive force, [52].

2.3 Properties of fluids

A system's features are referred to as its properties. A system is characterized as a group of objects having an established identity that interact with their environment. Here, fluid is taken to be a uniform, continuous substance devoid of small pores, [52].

2.3.1 Dimensions and Units

Dimensions are defined as the degree to which the physical quantity is expressed by raising the fundamental quantities. Mass, length, and time dimensions are denoted by the symbols $[M]$, $[L]$, and $[T]$, respectively. Units are the indeterminate magnitudes that are attributed to dimensions.

2.3.2 Density

Density is a term used to express the relationship between the volume (or amount of space) occupied by an item or substance and its mass (or quantity of stuff it contains). Density can be expressed as ρ,

$$\rho = \frac{mass}{volume} = \frac{m}{V}.$$

SI unit for density is $\frac{kg}{m^3}$ and dimension is $[ML^{-3}]$, [53].

2.3.3 Pressure

Pressure is the force that a thing applies to another. The force exerted on the item is per unit Area and perpendicular to its surface, [53]. P is the one who represents it.

$$P = \frac{Force}{Area} = \frac{F}{A}.$$

SI unit of pressure is $\frac{N}{m^2}$ and dimension is $[ML^{-1}T^{-1}]$.

2.3.4 Specific Heat

Specific heat is the amount of heat energy required to increase the temperature of a substance by one degree for a unit mass. Constant pressure (C_p) and constant volume (C_v) are the two forms of specific temperatures, [53].

2.3.5 Thermal Conductivity

The capacity of a substance to transfer heat, or how well it permits heat flow under temperature gradients, is measured by its thermal conductivity, [53]. It is represented by k.

Greater values correspond to improved heat conduction.

$$k = \frac{QL}{A\Delta T},$$

here Q denotes flow of heat per unit time, Cross-sectional area is represented by A and ΔT represents difference in temperature. Thermal conductivity's SI unit is $\frac{kgm}{s^3 k}$.

2.3.6 Heat Flux

Heat flux is a measure of how much heat moves over a surface in a specific amount of time. It is the rate of heat transfer across a surface per unit area. It is represented by q. Watts per square meter ($\frac{W}{m^2}$) is the unit of measurement.

2.3.7 Thermal Diffusivity

A fundamental feature that characterizes a fluid's capacity to transfer heat in relation to its capacity to store thermal energy is called thermal diffusivity. It is defined as the thermal conductivity (k) is divided by the the product of the specific heat capacity and fluid's density (ρ) at constant pressure (C_p), represented by α.

$$\alpha = \frac{k}{\rho C_p}.$$

2.3.8 Viscous Dissipation

In fluid mechanics, [54] the term "viscous dissipation" describes the process by which internal friction in a moving fluid transforms mechanical energy into heat. It results from the dissipation of kinetic energy caused by viscous strains brought on by fluid velocity gradients. The terms that indicate the rate of energy dissipation per unit volume in various directions inside the fluid are used to mathematically characterize this process.

2.3.9 Viscosity

Fluid resistance to flow is measured by a property called viscosity. There are two types of viscosity. Dynamic and Kinematic Viscosity. The reluctance of one fluid layer to slide on top of another is known as dynamic viscosity. The fluid's dynamic viscosity is divided to its density is known as kinematic viscosity, [54].

μ represents dynamic viscosity. SI unit of dynamic viscosity is $\frac{Ns}{m^2}$ and its dimension is $[ML^{-1}T^{-1}]$.

Kinematic viscosity is represented by ν. SI unit of kinematic viscosity is $\frac{m^2}{s}$ and its dimension is $[L^2T^{-1}]$.

2.4 Newton Law of Viscosity

It asserts that the rate of shear strain and the shear stress on a fluid elementary layer are exactly proportionate [53]. The viscosity coefficient is the same as the proportionality constant. Mathematically, it is expressed as

$$\tau = \mu \frac{du}{dy},$$

where τ represent shear stress, dynamic viscosity is represented by μ and $\frac{du}{dy}$ is the gradient of velocity perpendicular to flow direction.

2.5 Newtonian fluids

Newtonian fluids can have constant viscosity, and there is a linear and direct relationship between shear stress and deformation rate. Newtonian behavior is observed in fluids where particle interaction does not influence flow behavior. Examples are water and air [53].

2.6   Non-Newtonian Fluids

Non-Newtonian fluids have variable viscosity according to their situation and stress-deformation rate nonlinear connection, [53]. These fluids are also known as second-grade fluids. These fluids change their flow behavior under different conditions. Examples are toothpaste and ketchup.

2.7   Navior Stocks Equation

The Navier-Stokes equations determine how fluid materials move.The flow of compressible and incompressible fluids is governed by a system of nonlinear partial differential equations. The equations have the names of the two individuals who independently created them during the 1800s: George Gabriel Stokes and Claude-Louis Navier.
Mathematically,

$$\rho \left(\frac{\partial \boldsymbol{v}}{\partial t} + \boldsymbol{v}.\boldsymbol{\nabla v} \right) = -\boldsymbol{\nabla}p + \mu\boldsymbol{\nabla}^2\boldsymbol{v} + f,$$

where, ρ denotes density, $\boldsymbol{v}$ represents velocity vector, p be the pressure and f represents external force acting on a fluid, [54].

2.8   Law of Conservation of mass

The law of mass conservation in fluid mechanics explains that the total mass of a fluid passing through a closed system does not change over time. According to this theory, mass can only change in form or be redistributed within the system—it cannot be generated or lost. When examining fluid flow processes, it acts as a fundamental guideline that guarantees mass continuity throughout the system, [52].

2.9   Law of Conservation of energy

According to fluid mechanics, the total energy in a closed system of moving fluid stays

constant throughout time. This is known as the law of conservation of energy. Although energy can take on several forms, such as kinetic, potential, or internal energy, its overall value never changes. This idea directs fluid flow investigations, making sure that energy transformations are taken into consideration in computations and models, [54].

2.10   Velocity Field

In a given space, the distribution of particle or fluid element velocities is described by a velocity field. Every point in the field is represented by a vector that shows the motion's direction and speed. Fields are crucial to several branches of physics, including as general relativity, quantum physics, and electromagnetic. In many branches of research and engineering, these mathematical domains may be utilized to represent and examine physical phenomena. There are three types of fields. Scalar, vector and tensor fields.

2.10.1 Scalar Field

A scalar field describes the distribution of a scalar quantity by giving each point in a space a single numerical value. Scalar quantity is one which have only magnitude. Scalar fields are essential to the representation of scalar characteristics in fluid mechanics, such as temperature and pressure.

Since they provide a thorough understanding of the distribution of these variables within a fluid. They support forecasts and optimizations in a variety of engineering applications by assisting in the analysis of fluid flow.

2.10.2 Vector Field

A vector field shows the variation in space as well as the direction of an intrinsic property, such force or velocity, by assigning a vector to each point in a given region. Vector field have both magnitude and direction. Vector fields are important for the study of fluid mechanics because they allow the representation and analysis of fluid forces, velocities, and flow patterns.

They make it easier to comprehend fluid behavior, which helps with the design and improvement of technical applications like fluid flow in pipes and aerodynamics.

2.10.3 Tensor Field

A mathematical concept called a tensor field, which gives a tensor to every point in a space, is frequently used to simulate and examine the distribution of physical variables in several dimensions. Tensor fields are used in fluid mechanics to characterize and examine intricate physical phenomena including fluid flow, stress, and strain. They offer a thorough depiction of the spatial variation and interplay of various variables inside a fluid.

2.11   Stress

The force per unit area that fluid particles apply to a surface inside the fluid is referred to as stress. External pressures applied to an object within the material itself might result in stress. It is made up of normal stress, which operates perpendicular to the surface, and shear stress, which acts parallel to the surface, giving information on the distribution and influence of forces in the fluid. Stress is represented by σ.

$$Stress = \sigma = \frac{Force}{Area}.$$

The SI unit of stress is $\frac{N}{m^2}$, [54].

2.11.1 Cauchy Stress Tensor

The stress within a material at a particular position is described by the Cauchy stress tensor. It is essential for assessing and forecasting the mechanical behavior of materials under diverse circumstances and pertains to the force per unit area operating on numerous planes at that moment. The components of Cauchy stress tensor represents normal and shear stresses, [54].

2.11.2 Extra Stress Tensor

In fluid mechanics, the extra stress tensor is especially employed to account for additional stress contributions caused by fluid motion, [54]. The constitutive equations that control the connection between stress and strain in a fluid frequently include the extra strain tensor.

2.12   Flow

"Flow" in fluid mechanics describes the movement of a fluid, which can be either a liquid or a gas, [54]. Understanding fluid flow is essential to comprehending how fluids behave and interact with their environment. Analysis of the fluid's temperature, pressure, density, and velocity distributions as well as the forces and energy involved in the fluid's motion are all part of the study of fluid flow.

2.12.1 Stream line

Imaginary lines called streamlines show the routes taken by fluid particles as they pass through a fluid. The direction of the fluid velocity at any given position is indicated by the tangent to the streamline [54].

2.12.2 Steady Flow

Fluid flow that exhibits constant velocity, pressure, and other flow rates over time is referred to as steady flow. Every area of the flow experiences homogeneous fluid properties and a steady flow rate, and the parameters of the flow are stable throughout time. An accurate estimate for fluid systems in equilibrium is steady flow, [54].

2.12.3 Unsteady flow

Unsteady flow is the one in which properties like velocity, pressure are vary with time. It involves periodic fluctuations, happening throughout dynamic processes, temporary situations, or exogenous disruptions, comparing with steady flow when fluid characteristics stay constant over time, [54].

2.12.4 Laminar Flow

Laminar flow is a kind of fluid flow where the fluid moves smoothly or along predictable patterns. It usually occurs in small, very viscous pipelines with low fluid velocity. It is characterized by a constant, regular flow that is usually seen at low speeds and in circumstances when the fluid's viscosity outweighs the effects of inertial forces, [54].

2.12.5 Turbulent flow

According to fluid mechanics, turbulent flow is the chaotic, erratic movement of fluid particles characterized by variations in density, pressure, and velocity. When inertial forces outweigh viscosity, it often occurs at greater velocities and involves intricate vortices, eddies, and mixing between neighboring layers, [54].

2.12.6 Uniform Flow

In fluid mechanics, a fluid motion that is steady and constant with a velocity that doesn't change over time or across a cross-section is referred to as uniform flow. For conceptual ease, this condition—which assumes a constant density—is frequently employed in fluid mechanics investigations as a simplifying assumption. Uniform flow is appropriate for long straight lengths in open-channel flows with little acceleration or deceleration effects, [54].

2.12.7 Non-Uniform flow

Non-uniform flow describes a situation in which the fluid's velocity changes at various points within the flow, either throughout the cross-sectional area or along the channel's length. Non-uniform flow involves variations in pressure, density, and/or velocity over time and space. This kind of flow is typical in natural water courses, pipes that have varying diameters, and other scenarios where fluid velocity is affected by friction, obstructions, or geometric changes, [54].

2.12.8 Compressible flow

Compressible flow refers to major variations in temperature, pressure, and density which impact the fluid's volume. For high-speed situations such as aerodynamics, compressibility effects become significant, whereas incompressible flow implies small density fluctuations. This is why this kind of flow is important. Understanding compressible flow is very important when examining how gases behave while traveling at high speeds, [52].

2.12.9 Incompressible flow

Incompressible flow describes the flow of a fluid in which small variations in density occur. The fluid's density keeps almost constant in these flows, and changes in temperature and pressure rarely affect the fluid's volume. Incompressible flow is frequently used to analyze low-speed gas flows or liquid flows, which makes mathematical computations easier to understand and offers a helpful approximation in a variety of fluid dynamics and engineering settings, [52].

2.13   Heat Transfer

In fluid mechanics, the act of transferring thermal energy between two fluid regions a liquid or a gas or between a fluid and its solid boundaries is referred to as heat transfer. Numerous technical applications, including as the design and analysis of heat exchangers, boilers, cooling systems, and many other thermal systems, depend heavily on this phenomena, [53].

There are three modes of heat transfer.

2.13.1 Conduction

Thermal energy can move through a material or between two materials that are in direct contact when using this type of heat transfer, [53]. Conduction happens in fluids but is typically less important than in solids. For instance, heat conduction can occur across solid-fluid boundaries or within a fluid.

2.13.2 Convection

Convection is the movement of fluid particles carrying heat, and can be forced by external sources like fans or pumps, or it can happen naturally as a result of floatability brought on by temperature changes.

2.13.3 Radiation

Heat is transferred by electromagnetic waves and is known as radiation. Despite not needing a solid medium to propagate, fluid systems can nonetheless experience it. Thermal radiation is both absorbed and emitted by fluids. Radiation may become an important heat transmission method in some situations, such as hot regions.

2.14   Dimensionless numbers

2.14.1 Prandtl number

The Prandtl number Pr, which is dimensionless in fluid mechanics, indicates how important thermal diffusivity is in relation to momentum diffusivity (viscosity) in a fluid. It bears Ludwig Prandtl's name, a German scientist and engineer.

$$\text{Prandtl number} = \frac{\text{kinematic viscosity}}{\text{Thermal diffusitivity}},$$

$$Pr = \frac{\nu}{\alpha_f} = \frac{\mu/\rho}{k/\rho C_p},$$

$$Pr = \frac{\mu C_p}{k}.$$

2.14.2 Reynolds number

In fluid mechanics, the Reynolds number, or Re, is a dimensionless variable that is used to forecast flow patterns in various fluid flow scenarios. It bears the name of Osborne Reynolds, an Irish physicist who first proposed the idea. The Reynolds number, which is a measure of the ratio of viscous to inertial forces, aids in identifying the laminar, transitional, or turbulent flow type inside a fluid. Viscous forces

$$\text{Reynolds number} = \frac{\text{Inertial forces}}{\text{Viscous forces}},$$

$$Re = \frac{\rho v^2/L}{\mu v/L} = \frac{vL}{\nu}.$$

2.14.3 Eckert number

The Eckert number (Ec) represents the ratio of kinetic energy to enthalpy change in a fluid flow, a dimensionless metric. It can be defined as the relationship between the fluid's kinetic energy and the convective heat transfer rate. The Eckert number is helpful in examining how kinetic energy affects heat transfer and is frequently used in research involving high-speed flows.

$$Ec = \frac{c^2}{C_p T_0}.$$

2.14.4 Brinkman number

In the processing of polymers, the Brinkman number (Br) is a dimensionless quantity that is associated with heat transfer through a wall to a viscous fluid in motion, [54]. It bears the

name Henri Brinkman in honor of the Dutch mathematician and scientist.

$$Br = \frac{\mu u^2}{k(T_w - T_0)} = PrEc,$$

where μ, k, T_w, T_0 are dynamic viscosity, thermal conductivity, wall temperature and bulk fluid temperature.

2.15 Basic Equations:

2.15.1 Equation of Continuity:

According to the continuity equation, the rate of mass flow into and out of a particular region, plus any buildup within the zone, must equal one another.
Mathematically,

$$\nabla.(\rho V) + \frac{\partial \rho}{\partial t} = 0.$$

For incompressible fluids, when density remains constant.

$$\nabla.V = 0.$$

2.15.2 Momentum Equation

This equation is derived from Newton 2nd law of motion. According to this equation, an object's net force is equal to the product of its mass and acceleration, [53].

The momentum equation for an incompressible fluid can be expressed as

$$\rho \frac{dv}{dt} = div\tau + pb.$$

$\rho \frac{dv}{dt}$ represents local rate of change of momentum with time. $div\tau$ represents surface force and

pb represents body force.

2.15.3 Energy Equation

It is derived from first law of thermodynamics. This law states that "The quantity of heat energy introduced to a thermodynamic system less the work the system does on its surroundings is the increase in internal energy of the system", [53].

$$\rho C_p \frac{dT}{dt} = -div\ \boldsymbol{q} + \boldsymbol{\tau}.\boldsymbol{l}.$$

$\rho C_p \frac{dT}{dt}$ represents total internal energy, $-div\ \boldsymbol{q}$ represents heat flux, $\boldsymbol{\tau}.\boldsymbol{l}$ denotes viscous dissipation.

2.16 Perturbation Method

Perturbation method is used to estimate solutions to problems that are hard to solve directly. These techniques have two main applications. First, simulating real-world applications like high Reynolds number flow that inherently provide such a small parameter. One of the main reasons perturbation methods are a mainstay of applied mathematics is that this type of application is rather widespread.

In addition with numerical techniques, perturbation methods are used in a second way. There are two main disadvantages to numerical calculation, despite the fact that computed solutions to a problem can be quite accurate and available for very complicated systems; perturbation methods can assist with both of them.

When performing numerical computations, there is always a chance that the code is incorrect. One useful check is to drive one or more of the problem's physical parameters to extreme values and contrast the numerical outcomes with a perturbation solution calculated when that parameter is small (or large).

CHAPTER 3

MHD Peristaltic Transport of Eyring-Powell Fluid with Heat/Mass Transfer, Wall Properties and Slip Conditions

3.1 Introduction

This chapter provides a detailed review of the research work done by S.Hina [55]. The objective of this work was to investigate the influence of mass and heat transfer occurring simultaneously on the peristaltic transport of Eyring-Powell fluid while taking slip effects and wall features into account. The problem formulation also takes into account viscous dissipation effects. A regular perturbation strategy is used to derive the series solutions of the generated differential systems. The heat transfer coefficient, stream function, temperature, axial velocity, and concentration are obtained, and the findings are described graphically.

3.2 Mathematical Formulation

This paper showed how heat and mass transfer affect Eyring-Powell fluid peristaltic flow in a $2d_1$ wide channel. The study takes into account the concentration slip, temperature jump condition, and velocity slip. The velocity is made up of two components: v is the transverse element in the y-direction and u is the axial element in the x-direction. The wave's shape develops alongside the walls:

$$y^* = \pm\eta(x^*, t^*) = \pm\left[d_1 + a\sin\frac{2\pi}{\lambda}(x^* - ct^*)\right], \tag{3.1}$$

where, d_1 stands for the mean half of the channel's width, λ for the wavelength, c for the velocity of peristaltic wave, and t for the time.

Shear in non-Newtonian flow is studied using the Eyring-Powell fluid model.

The fluid model of Eyring-Powell has a stress tensor that is

$$\tau = \left[\mu + \frac{1}{\beta\dot{\gamma}}\sinh^{-1}\left(\frac{1}{c_1}\dot{\gamma}\right)A_1\right], \tag{3.2}$$

$$\dot{\gamma} = \sqrt{\frac{1}{2}tr(A_1)^2}, \qquad A_1 = (grad\ V) + (grad\ V)^T, \tag{3.3}$$

where $\sinh^{-1}$ can be expanded upto second order.

$$\sinh^{-1}\left(\frac{1}{c_1}\gamma\right) \cong \frac{\gamma}{c_1} - \frac{\gamma^3}{6c_1^3}, \qquad \frac{\gamma^5}{c_1^5} << 1 \tag{3.4}$$

here, β and c_1 are the Eyring-Powell fluid parameters, while μ is the dynamic viscosity.

$$\text{grad}\ V = \begin{bmatrix} \frac{\partial u^*}{\partial x^*} & \frac{\partial u^*}{\partial y^*} \\ \frac{\partial v^*}{\partial x^*} & \frac{\partial v^*}{\partial y^*} \end{bmatrix} \qquad \text{and} \qquad (grad\ V)^T = \begin{bmatrix} \frac{\partial u^*}{\partial x^*} & \frac{\partial u^*}{\partial y^*} \\ \frac{\partial v^*}{\partial x^*} & \frac{\partial v^*}{\partial y^*} \end{bmatrix}^T \tag{3.5}$$

$$A_1 = \begin{bmatrix} 2\frac{\partial u^*}{\partial x^*} & \frac{\partial u^*}{\partial y^*} + \frac{\partial v^*}{\partial x^*} \\ \frac{\partial v^*}{\partial x^*} + \frac{\partial u^*}{\partial y^*} & 2\frac{\partial v^*}{\partial y^*} \end{bmatrix}, \tag{3.6}$$

$$\gamma = \sqrt{2\left(\frac{\partial u^*}{\partial x^*}\right)^2 + \left(\frac{\partial u^*}{\partial y^*} + \frac{\partial v^*}{\partial x^*}\right)^2 + 2\left(\frac{\partial v^*}{\partial y^*}\right)^2}. \tag{3.7}$$

The components of stress tensor are

$$\tau_{x^*x^*} = \left(\mu + \frac{1}{\beta c_1}\right)\frac{\partial u^*}{\partial x^*} - \frac{2}{6\beta c_1^3}\left[2\left(\frac{\partial u^*}{\partial x^*}\right)^3 + \frac{\partial u^*}{\partial x^*}\left(\frac{\partial u^*}{\partial y^*} + \frac{\partial v^*}{\partial x^*}\right)^2 + 2\frac{\partial u^*}{\partial x^*}\left(\frac{\partial v^*}{\partial y^*}\right)^2\right], \tag{3.8}$$

$$\tau_{x^*y^*} = \left(\mu + \frac{1}{\beta c_1}\right)\left(\frac{\partial u^*}{\partial y^*} + \frac{\partial v^*}{\partial x^*}\right) - \frac{1}{6\beta c_1^3}\left[2\left(\frac{\partial u^*}{\partial x^*}\right)^2\left(\frac{\partial u^*}{\partial y^*} + \frac{\partial v^*}{\partial x^*}\right) + \left(\frac{\partial u^*}{\partial y^*} + \frac{\partial v^*}{\partial x^*}\right)^3 + 2\left(\frac{\partial v^*}{\partial y^*}\right)^2\left(\frac{\partial u^*}{\partial y^*} + \frac{\partial v^*}{\partial x^*}\right)\right],$$

(3.9)

$$\tau_{y^*y^*} = 2\left(\mu + \frac{1}{\beta c_1}\right)\frac{\partial v^*}{\partial y^*} - \frac{2}{6\beta c_1^3}\left[2\left(\frac{\partial v^*}{\partial y^*}\right)^3 + \frac{\partial v}{\partial y^*}\left(\frac{\partial u^*}{\partial y^*} + \frac{\partial v^*}{\partial x^*}\right)^2 + 2\frac{\partial v^*}{\partial y^*}\left(\frac{\partial u^*}{\partial x^*}\right)^2\right].$$

(3.10)

The governing equations to describe the flow problem for the fluid model Eyring-Powell is provided as

Equation of continuity is given as :

$$\frac{\partial u^*}{\partial x^*} + \frac{\partial v^*}{\partial y^*} = 0,$$

(3.11)

The x-component of momentum equation is given as

$$\rho\left(\frac{\partial u^*}{\partial t^*} + u^*\frac{\partial u^*}{\partial x^*} + v\frac{\partial u^*}{\partial y^*}\right) = -\frac{\partial p^*}{\partial x^*} + \left(\mu + \frac{1}{\beta c_1}\right)\left(\frac{\partial^2 u^*}{\partial x^{*2}} + \frac{\partial^2 u^*}{\partial y^{*2}}\right)$$

$$- \frac{1}{3\beta c_1^3}\frac{\partial}{\partial x^*}\left[\left\{2\left(\frac{\partial u^*}{\partial x^*}\right)^2 + 2\left(\frac{\partial v^*}{\partial y^*}\right)^2 + \left(\frac{\partial u^*}{\partial y} + \frac{\partial v^*}{\partial x^*}\right)^2\right\}\frac{\partial u^*}{\partial x^*}\right]$$

$$- \frac{1}{6\beta c_1^3}\frac{\partial}{\partial y^*}\left[\left\{2\left(\frac{\partial u^*}{\partial x^*}\right)^2 + 2\left(\frac{\partial v^*}{\partial y^*}\right)^2 + \left(\frac{\partial u^*}{\partial y^*} + \frac{\partial v^*}{\partial x^*}\right)^2\right\}\left(\frac{\partial u^*}{\partial y^*} + \frac{\partial v^*}{\partial x^*}\right)\right] - \sigma\beta_0^2 u,$$

(3.12)

The y-component of momentum equation is as under

$$\rho\left(\frac{\partial v^*}{\partial t^*} + u^*\frac{\partial v^*}{\partial x^*} + v^*\frac{\partial v^*}{\partial y^*}\right) = -\frac{\partial p^*}{\partial y^*} + \left(\mu + \frac{1}{\beta c_1}\right)\left(\frac{\partial^2 v}{\partial x^{*2}} + \frac{\partial^2 v^*}{\partial y^{*2}}\right)$$

$$- \frac{1}{3\beta c_1^3}\frac{\partial}{\partial y^*}\left[\left\{2\left(\frac{\partial u^*}{\partial x^*}\right)^2 + 2\left(\frac{\partial v^*}{\partial y^*}\right)^2 + \left(\frac{\partial u^*}{\partial y^*} + \frac{\partial v^*}{\partial x^*}\right)^2\right\}\frac{\partial v^*}{\partial x^*}\right]$$

$$- \frac{1}{6\beta c_1^3}\frac{\partial}{\partial y^*}\left[\left\{2\left(\frac{\partial u^*}{\partial x^*}\right)^2 + 2\left(\frac{\partial v^*}{\partial y}\right)^2 + \left(\frac{\partial u^*}{\partial y^*} + \frac{\partial v^*}{\partial x^*}\right)^2 +\right\}\left(\frac{\partial u^*}{\partial y^*} + \frac{\partial v^*}{\partial x^*}\right)\right],$$

(3.13)

The energy equation is given as below

$$\rho C_p \left(\frac{\partial T}{\partial t^*} + u \frac{\partial T}{\partial x^*} + v \frac{\partial T}{\partial y^*} \right) = k \left(\frac{\partial^2 T}{\partial x^{*2}} + \frac{\partial^2 T}{\partial y^{*2}} \right) + \left(\mu + \frac{1}{\beta c_1} \right) \left[4 \left(\frac{\partial u^*}{\partial x^*} \right)^2 + \left(\frac{\partial u^*}{\partial y^*} + \frac{\partial v^*}{\partial x^*} \right)^2 \right]$$

$$- \frac{2}{3 \beta c_1^3} \left(\frac{\partial u^*}{\partial x^*} \right)^2 \left\{ 2 \left(\frac{\partial u^*}{\partial x^*} \right)^2 + 2 \left(\frac{\partial v^*}{\partial y^*} \right)^2 + \left(\frac{\partial u^*}{\partial y^*} + \frac{\partial v^*}{\partial x^*} \right)^2 \right\}$$

$$- \frac{1}{6 \beta c_1^3} \left(\frac{\partial u^*}{\partial y^*} + \frac{\partial v^*}{\partial x^*} \right)^2 \left\{ 2 \left(\frac{\partial u^*}{\partial x^*} \right)^2 + 2 \left(\frac{\partial v^*}{\partial y^*} \right)^2 + \left(\frac{\partial u^*}{\partial y^*} + \frac{\partial v^*}{\partial x^*} \right)^2 \right\}, \qquad (3.14)$$

And the concentration equation is described as

$$\frac{\partial C}{\partial t^*} + u^* \frac{\partial C}{\partial x^*} + v^* \frac{\partial C}{\partial y^*} = D \left(\frac{\partial^2 C}{\partial x^{*2}} + \frac{\partial^2 C}{\partial y^{*2}} \right) + \frac{D K_T}{T_m} \left(\frac{\partial^2 T}{\partial x^{*2}} + \frac{\partial^2 T}{\partial y^{*2}} \right). \qquad (3.15)$$

Here ρ is the density, Electrical conductivity of fluid is represented by σ, β_0 represents applied magnetic field, C_p is specific heat, D is the coefficient of mass diffusivity, T_m is the mean temperature, K_T thermal diffusion ratio, C is concentration of fluid.

The boundary conditions are of the form

$$\frac{\partial}{\partial x} \left(\tau \frac{\partial^2}{\partial x^{*2}} + m \frac{\partial^2}{\partial t^{*2}} + d \frac{\partial}{\partial t} \right) \eta = \left(\mu + \frac{1}{\beta c_1} \right) \left(\frac{\partial^2 u^*}{\partial x^{*2}} + \frac{\partial^2 u^*}{\partial y^{*2}} \right) - \sigma \beta_0^2 u^* -$$

$$\rho \left(\frac{\partial u^*}{\partial t} + u \frac{\partial u^*}{\partial x} + v^* \frac{\partial u^*}{\partial y^*} \right) - \frac{1}{6 \beta c_1^3} \frac{\partial}{\partial y^*} \left[\left\{ 2 \left(\frac{\partial u^*}{\partial x^*} \right)^2 + 2 \left(\frac{\partial v^*}{\partial y^*} \right)^2 + \left(\frac{\partial u^*}{\partial y^*} + \frac{\partial v^*}{\partial x^*} \right)^2 \right\} \left(\frac{\partial u^*}{\partial y^*} + \frac{\partial v^*}{\partial x^*} \right) \right]$$

$$- \frac{1}{3 \beta c_1^3} \frac{\partial}{\partial x^*} \left[\left\{ 2 \left(\frac{\partial u^*}{\partial x^*} \right)^2 + 2 \left(\frac{\partial v^*}{\partial y^*} \right)^2 + \left(\frac{\partial u^*}{\partial y^*} + \frac{\partial v^*}{\partial x^*} \right)^2 \right\} \frac{\partial u^*}{\partial x^*} \right], \qquad at \ y^* = \pm \eta, \qquad (3.16)$$

$$\mu \pm \beta_1 \left(\frac{\partial u^*}{\partial y^*} + \frac{\partial v^*}{\partial x^*} \right) \left[\left(\mu + \frac{1}{\beta c_1} \right) - \frac{1}{6 \beta c_1^3} \left\{ 2 \left(\frac{\partial u^*}{\partial x^*} \right)^2 + 2 \left(\frac{\partial v^*}{\partial y^*} \right)^2 + \left(\frac{\partial u^*}{\partial y^*} + \frac{\partial v^*}{\partial x^*} \right)^2 \right\} = 0 \right] \ at \ y^* = \pm \eta, \quad (3.17)$$

$$T \pm \beta_2 \frac{\partial T}{\partial y} = T_0, \quad C \pm \beta_3 \frac{\partial C}{\partial y} = C_0 \qquad at \quad y^* = \pm \eta, \qquad (3.18)$$

where τ is elastic tension, d is wall damping coefficient, m is plate mass per unit area, T_0, C_0 are temperature and concentration at walls, $\beta_1, \beta_2, \beta_3$ are temperature, concentration and velocity slips.

Let us now provide the stream function ψ^* as

$$u = \frac{\partial \psi^*}{\partial y^*}, \qquad v^* = -\frac{\partial \psi^*}{\partial x^*},$$

and the dimensionless quantities are:

$$x = \frac{x^*}{\lambda}, y = \frac{y^*}{d_1}, \psi = \frac{\psi^*}{cd_1}, t = \frac{ct^*}{\lambda}, p = \frac{p^* d_1^2}{c\lambda\mu}, B = \frac{1}{\mu\beta c_1}, \delta = \frac{d_1}{\lambda},$$

$$A = \frac{Bc^2}{2d_1^2 c_1^2}, Re = \frac{\rho c d_1}{\mu}, \theta = \frac{T - T_0}{T_0}, M^2 = \sqrt{\frac{\sigma}{\mu}} B_0 d_1, Pr = \frac{\mu C_P}{\kappa},$$

$$Ec = \frac{c^2}{C_p T_0}, E_1 = -\tau \frac{d_1^3}{\lambda^3 \mu c}, E_2 = \frac{mcd_1^3}{\lambda^3 \mu}, E_3 = \frac{dd_1^3}{\lambda^2 \mu}, \beta_i^* = \frac{\beta_i}{d_1} \ (i = 1 - 3)$$

$$S_c = \frac{\mu}{D_\rho}, \in = \frac{a}{d_1} S_r = \frac{\rho D K_T T_0}{\mu T_m C_o}. \tag{3.19}$$

The Eyring-Powell fluid model's material parameters are B and A, Wave number is represented by δ, wall elastance measure E_1, parameter of mass per unit area is E_2, and wall damping value is E_3. Prandtl number (Pr), Eckert number (Ec), Schmidt (Sc), Soret (Sr), Reynolds (Re) are all dimensionless numbers and temperature distribution and mass concentration are given by θ and φ respectively.

Once the stream function is introduced, the continuity equation is immediately met. First, we non-dimensionalize the system and then apply the lubrication approach. The rulling equations are reduced in following factors.

$$\frac{\partial p}{\partial x} = (1 + B)\frac{\partial^3 \psi}{\partial y^3} - \frac{A}{3}\frac{\partial}{\partial y}\left(\frac{\partial^2 \psi}{\partial y^2}\right)^3 - M^2 \frac{\partial \psi}{\partial y}, \tag{3.20}$$

$$\frac{\partial p}{\partial y} = 0, \tag{3.21}$$

$$\frac{1}{Pr}\frac{\partial^2\theta}{\partial y^2} + Ec(\frac{\partial^2\psi}{\partial y^2})^2 \left[(1+B) - \frac{A}{3}\left(\frac{\partial^2\psi}{\partial y^2}\right)^2\right] = 0, \tag{3.22}$$

$$\frac{\partial^2\varphi}{\partial y^2} + ScSr\frac{\partial^2\theta}{\partial y^2} = 0, \tag{3.23}$$

and the boundary conditions are:

$$\frac{\partial}{\partial x}\left(E_1\frac{\partial^2}{\partial x^2} + E_2\frac{\partial^2}{\partial t^2} + E_3\frac{\partial}{\partial t}\right)\eta = (1+B)\frac{\partial^3\psi}{\partial y^3} - \frac{A}{3}\frac{\partial}{\partial y}\left(\frac{\partial^2\psi}{\partial y^2}\right)^3 - M^2\frac{\partial\psi}{\partial y}, \quad at\ y = \pm\eta \tag{3.24}$$

$$\frac{\partial\psi}{\partial y} \pm \beta_1\left[(1+B)\frac{\partial^2\psi}{\partial y^2} - \frac{A}{3}\left(\frac{\partial^2\psi}{\partial y^2}\right)^3\right] = 0, \theta \pm \beta_2\frac{\partial\theta}{\partial y} = 0, \varphi \pm \beta_3\frac{\partial\varphi}{\partial y} = 0\ at\ y = \pm\eta \tag{3.25}$$

Combing equations (3.20) and (3.21), we get the compatibility equation

$$(1+B)\frac{\partial^4\psi}{\partial y^4} - \frac{A}{3}\frac{\partial^2}{\partial y^2}\left(\frac{\partial^2\psi}{\partial y^2}\right)^3 - M^2\frac{\partial^2\psi}{\partial y^2} = 0. \tag{3.26}$$

3.3 Solution Methodology

To identify the system's solution involving the small Eyring-Powell fluid perimeter A, use the perturbation approach.

$$\psi = \psi_0 + A\psi_1 + O(A)^2 + \cdots, \tag{3.27}$$

$$\theta = \theta_0 + A\theta_1 + O(A)^2 + \dots, \tag{3.28}$$

$$\varphi = \varphi_0 + \varphi_1 + O(A)^2 + \dots \tag{3.29}$$

3.3.1 Zeroth Order System

$$(1 + B)\frac{\partial^4 \psi_0}{\partial y^4} - M^2 \frac{\partial^2 \psi_0}{\partial y^2} = 0, \tag{3.30}$$

$$\frac{1}{Pr}\frac{\partial^2 \theta_0}{\partial y^2} + Ec(1 + B)\left(\frac{\partial^2 \psi_0}{\partial y^2}\right)^2 = 0, \tag{3.31}$$

$$\frac{\partial^2 \varphi_0}{\partial y^2} + ScSr \frac{\partial^2 \theta_0}{\partial y^2} = 0, \tag{3.32}$$

with corresponding boundary conditions:

$$\frac{\partial}{\partial x}\left(E_1 \frac{\partial^2}{\partial x^2} + E_2 \frac{\partial^2}{\partial t^2} + E_3 \frac{\partial}{\partial t}\right)\eta = (1 + B)\frac{\partial^3 \psi_0}{\partial y^3} - \frac{A}{3}\frac{\partial}{\partial y}\left(\frac{\partial^2 \psi_0}{\partial y^2}\right)^3 - M^2 \frac{\partial \psi_0}{\partial y}, \quad at\ y = \pm\eta \tag{3.33}$$

$$\frac{\partial \psi_0}{\partial y} \pm \beta_1(1 + B)\frac{\partial^2 \psi_0}{\partial y^2} = 0, \theta_0 \pm \beta_2 \frac{\partial \theta_0}{\partial y} = 0, \varphi_0 \pm \beta_3 \frac{\partial \varphi_0}{\partial y} = 0 \quad at\ y = \pm\eta. \tag{3.34}$$

3.3.3 First Order System

$$(1 + B)\frac{\partial^4 \psi_1}{\partial y^4} - \frac{1}{3}\frac{\partial^2}{\partial y^2}\left(\frac{\partial^2 \psi_0}{\partial y^2}\right)^3 - M^2 \frac{\partial^2 \psi_1}{\partial y^2} = 0, \tag{3.35}$$

$$\frac{\partial^2 \theta_1}{\partial y^2} + 2Br(1 + B)\left(\frac{\partial^2 \psi_0}{\partial y^2}\frac{\partial^2 \psi_1}{\partial y^2}\right) - \frac{Br}{3}\left(\frac{\partial^2 \psi_0}{\partial y^2}\right)^4 = 0, \tag{3.36}$$

$$\frac{\partial^2 \varphi_1}{\partial y^2} + ScSr \frac{\partial^2 \theta_1}{\partial y^2} = 0, \tag{3.37}$$

and the corresponding boundary conditions:

$$(1+B)\frac{\partial^3\psi_1}{\partial y^3} - \frac{1}{3}\frac{\partial}{\partial y}\left(\frac{\partial^2\psi_0}{\partial y^2}\right)^3 - M^2\frac{\partial^2\psi_1}{\partial y^2} = 0 \quad at\ y = \pm\eta \tag{3.38}$$

$$\left.\begin{array}{c}\frac{\partial\psi_1}{\partial y} \pm \beta_1\left[(1+B)\frac{\partial^2\psi_1}{\partial y^2} - \frac{1}{3}\left(\frac{\partial^2\psi_1}{\partial y^2}\right)^3\right] = 0,\ \theta_1 \pm \beta_2\frac{\partial\theta_1}{\partial y} = 0,\\ \varphi_1 \pm \beta_3\frac{\partial\varphi_1}{\partial y} = 0 \ at\ y = \pm\eta.\end{array}\right\} \tag{3.39}$$

3.4 Results and Discussion:

The physical interpretation of parameter behavior as it relates to the velocity u, concentration distribution ϕ temperature distribution θ and stream function ϕ is the focus of this section. An intriguing phenomena known as "trapping" occurs when streamlines split and enclose to create a bolus that moves with the wave. The streamlines for a range of effective parameter values are shown in Figure 3.1–3.5. The conduct of various factors on the velocity profile u is plotted in Figure 3.6–3.10. To analyze the impacts of different parameters on the temperature distribution θ, Figure 3.11–3.17 are presented. To investigate the impact of factors on the concentration distributionϕ, Figure 3.18–3.25has been created.

The effect of the fluid parameter A on the streamlines is seen in Figures 3.1a and 3.1b. It has been shown that increasing A causes a rise in the quantity of circulations and the size of the trapped bolus. Additionally, it is discovered that the boluses in the top and bottom sides of the channel are comparable in size and shape. The effect of Eyring-Powell fluid parameter B on streamlines is shown in Figures 3.2a and 3.2b. The quantity and count of boluses seem to go up as B goes up for some fixed A. We can infer from Figs. 3.3a and *3.3b* that the amplitude ratio increases the quantity and count of boluses. When M is increased, the size of the bolus and the quantity of circulations decrease as shown in figures 3.4a and 3.4b. Additionally, it is discovered that bolus vanishes for a big enough Hartman number M. Figures 3.5a–3.5d demonstrate the influene of wall characteristics on stream functionality. It is noted that as wall flexibility E_1 and mass per unit area of wall E_2 are raised, the frequency of circulations increases and the bolus size increases.

The non-linear portion of the governing momentum equation appears when the Eyring-Powell fluid parameter A rises, the axial velocity increases, grows, as shown in Figure 3.6–3.10. The impact of Eyring-Powell fluid parameter B is shown in Figure 3.7. When B is increased, axial

velocity seems to decrease. The impacts of M on velocity profile are seen in Figure 3.8. The axial path of velocity is the diminishing function of M. A Resistive force applied to the magnetic field resists the flow in a transverse direction, resulting in a decrease in velocity. Figure 3.9 shows the influence of the velocity slip parameter β_1 on the axial velocity. The velocity slip parameter and the axial velocity profile are shown to be directly correlated. The slip effect's intensification reduces the channel walls' resistance, which finally causes the flow to accelerate. The impacts of wall characteristics on the axial velocity are seen in Figure 3.10. E_1, E_2 and E_3. The flow in the axial direction is found to decrease with increase in either wall mass per unit area E_2, wall elasticity E_1,wall damping valueE_3.

Figure 3.11–3.17 shows that the temperature in the channel's center is higher than that of the walls. In actuality, this is because the energy equation takes viscous dissipation effects into account. Figure 3.11 illustrates how temperature θ rises when Eyring-Powell fluid parameter A grows, while Figure 3.12 displays the same trend for parameter B. It is seen that as the velocity slip parameter β_1 and Hartman number M are increased, temperature rises (see Figures 3.13 and 3.14. Figures 3.15 and 3.16 show that when higher values of the Brinkman number Br and thermal slip parameter β_2 are taken into consideration, the temperature θ increases. The temperature profile shows the same behavior like velocity profile. Figure 3.17 represents that the temperature profile increases with an increase in both wall elasticity and wall mass per unit area whereas it has inverse relationship with the wall damping coefficient.

In contrast to the temperature θ, the concentration is lower in the center than it is at the walls. Figure 3.18 shows how concentration ϕ decreases when Eyring-Powell fluid parameter A grows, while Figure 3.19 displays the same trend for parameter B. As demonstrated in Figures 3.20 and 3.21, there is a modest drop in ϕ when the velocity slip parameter β_1 and with Hartman number M are increased.

In figure 3.22, As the concentration slip parameter β_3 increases, the concentration of species decrease. As seen in Figure 3.23, the behavior is viscous dissipation if the concentration is small. Figure 3.24 show that when we increase Sc number, concentration profile decreases. In a qualitative sense, wall attributes have the same influence on ϕ as they do on θ.
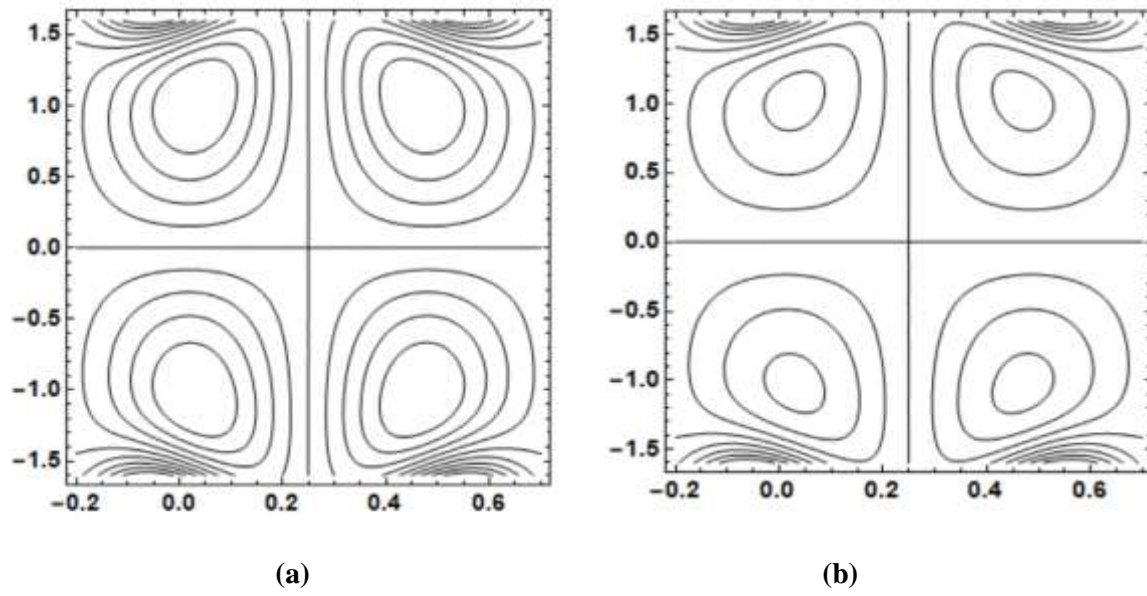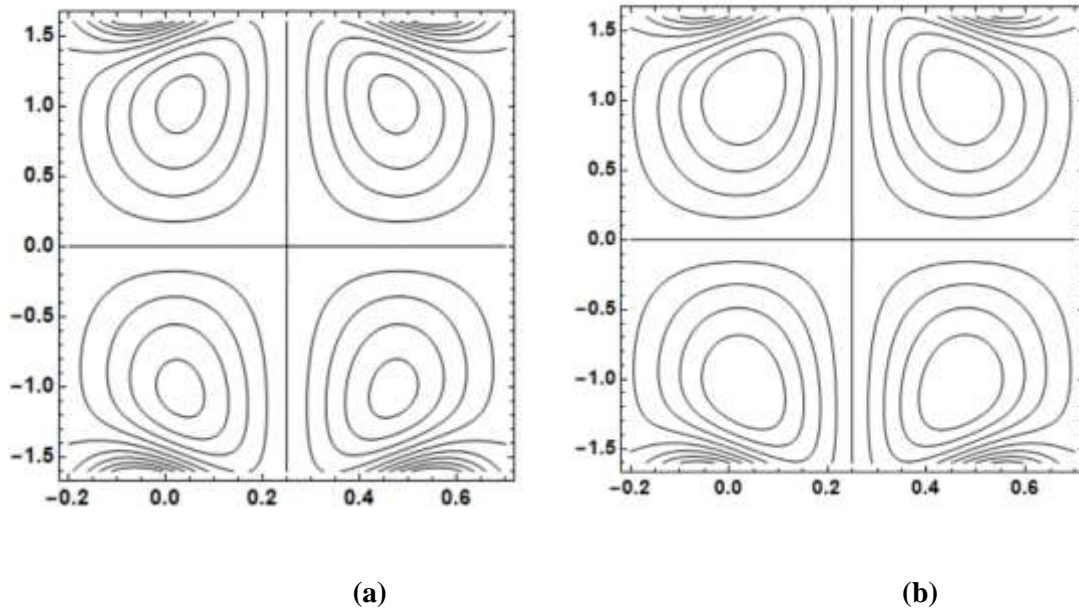
(a)   **(b)**
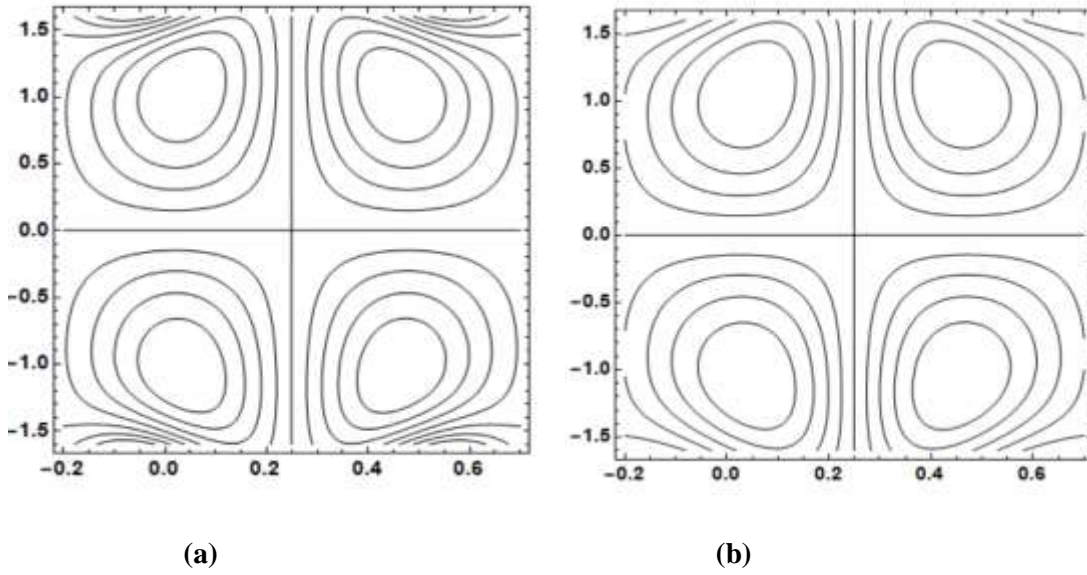
Figure 3.1 Variations of A on contours as E_1=0.2, E_2=0.1, E_3=0.01, t=0, M=2, β_1=0.01, $\epsilon = 0.15$, B=2 (a) A=0.1, (b) A=0.

(a)   **(b)**
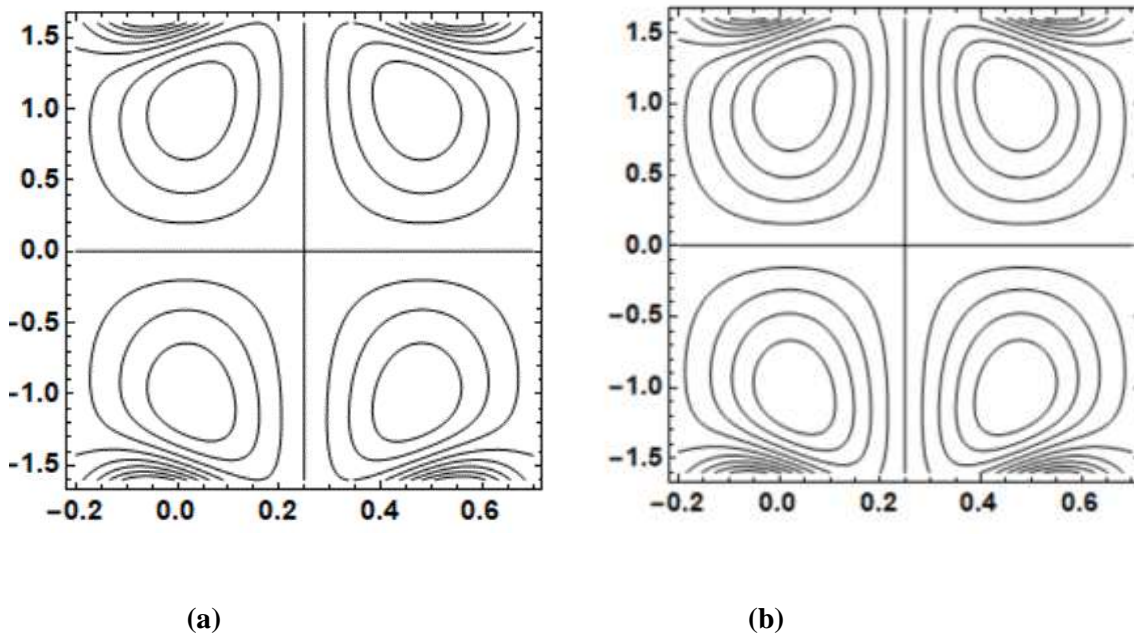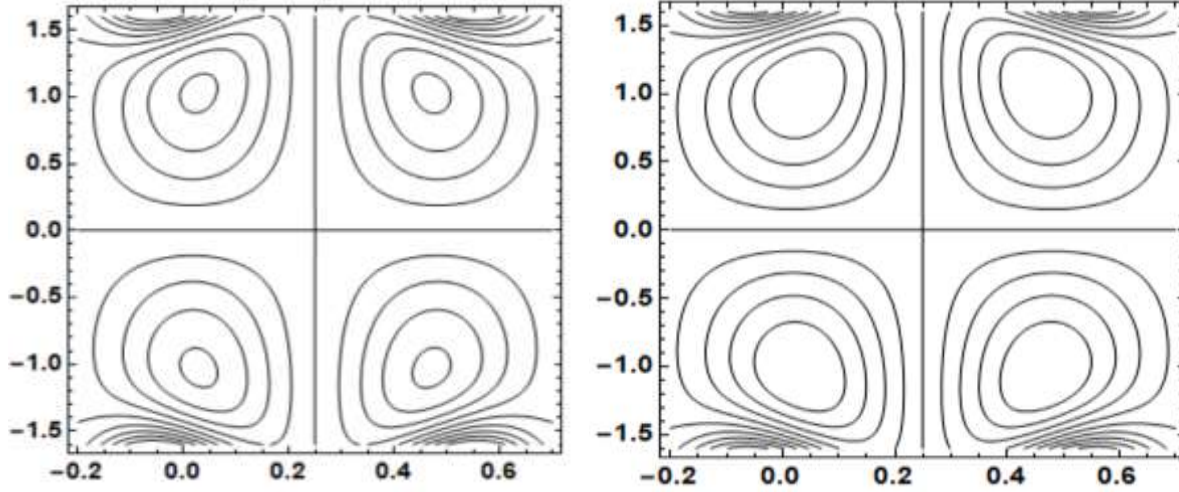
Figure 3.2 Variation of B on contours as $E_1 = 0.2$, $E_2 = 0.1$, $E_3 = 0.01$, t = 0, B = 2, $M = 2, \beta_1 = 0.01$, $\epsilon = 0.15$, A = 0.2 (a): B = 1.5 (b): B = 2.2.

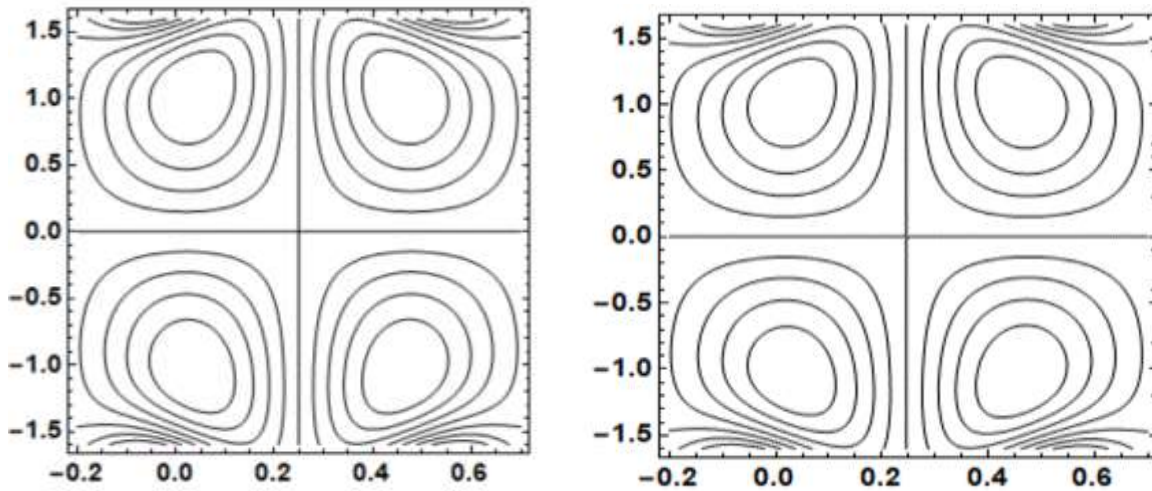**(a)**   **(b)**

Figure 3.3 Variation of M on contours as $E_1 = 0.2$, $E_2 = 0.1$, $E_3 = 0.01$, t = 0, A = 0.2, $\beta_1 = 0.01$, $\epsilon = 0.15$, B = 2 (a): M = 2.9 (b): M = 2.

(a)   **(b)**

Figure 3.4 Variation of β_1 on contours as $E_1 = 0.2$, $E_2 = 0.1$, $E_3 = 0.01$, M = 2, t = 0, A = 0.2, B = 2, M = 2, (a): $\beta_1 = 0$ (b): $\beta_1 = 0.03$.

(a)

(b)

(c)

(d)

Figure 3.5 Variation of wall properties on contours as t = 0, B = 2, M = 2, ϵ = 0.15, β_1 = 0.01, A = 0.1 (a): $E_1 = 0.2$, $E_2 = 0.3$, $E_3 = 0.01$, (b): $E_1 = 0.3$, $E_2 = 0.1$, $E_3 = 0.01$, (c): $E_1 = 0.2$, $E_2 = 0.1$, $E_3 = 0.01$, (d): $E_1 = 0.2$, $E_2 = 0.1$, $E_3 = 0.05$.
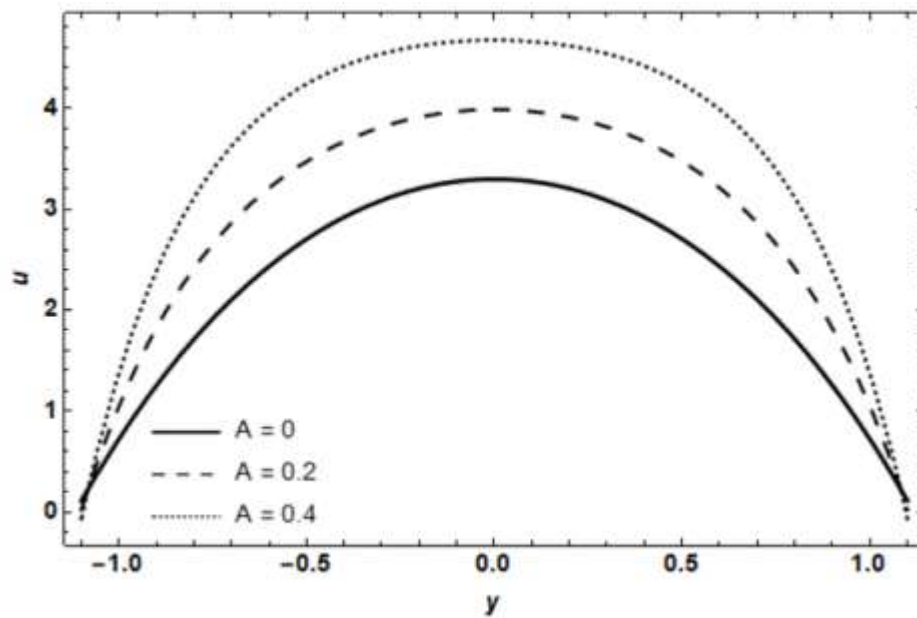
Figure 3.6 Variation of *A* on velocity field at *A= 0, 0.2, 0.04*
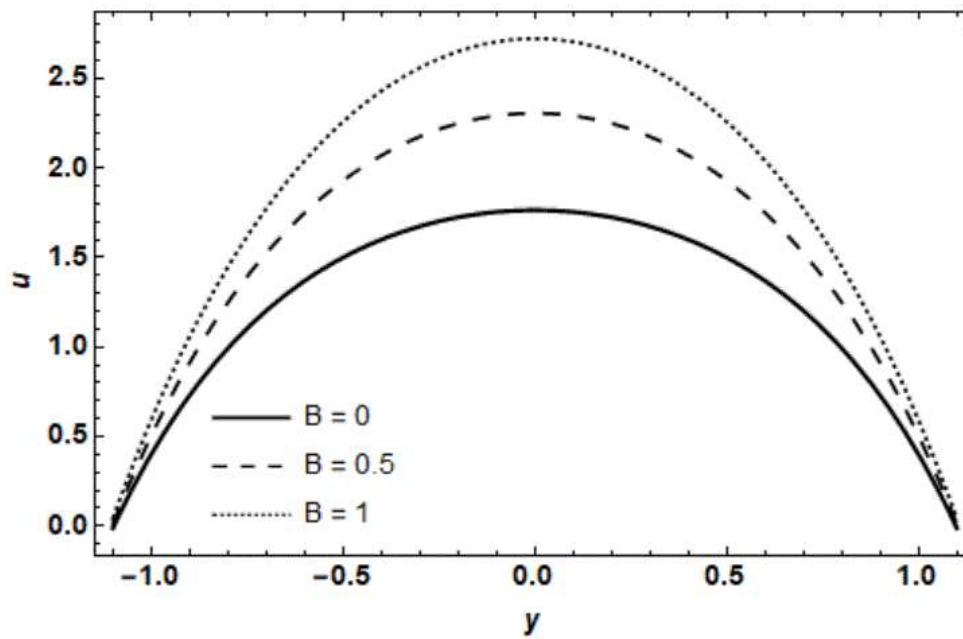
Figure 3.7 Variation of *B* on velocity field at *B= 0, 0.5,1*
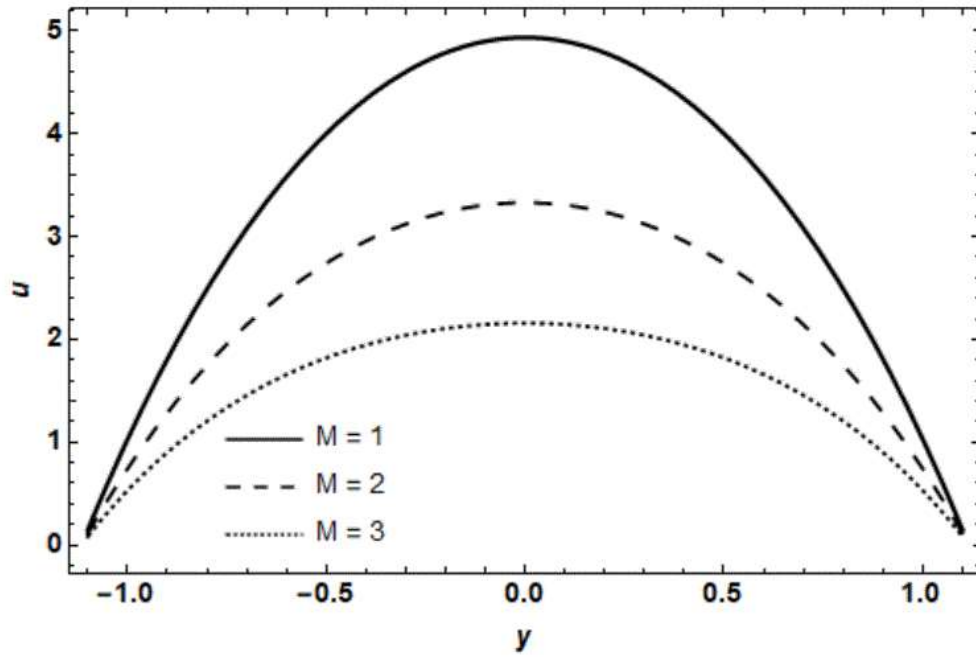
Figure 3.8 Variation of *M* on velocity field at *M= 1, 2, 3*
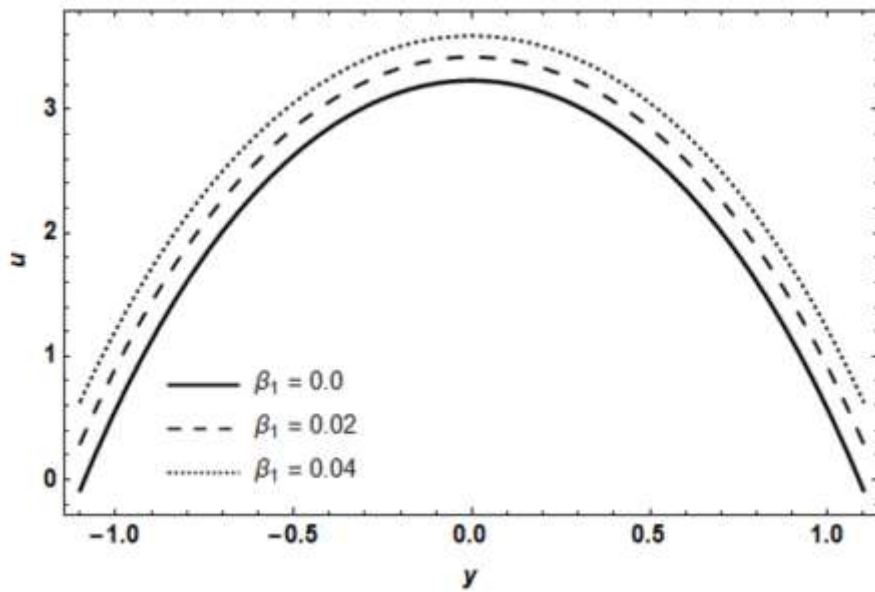
Figure 3.9 Variation of β_1 on velocity field at β_1= 0, 0.02, 0.04
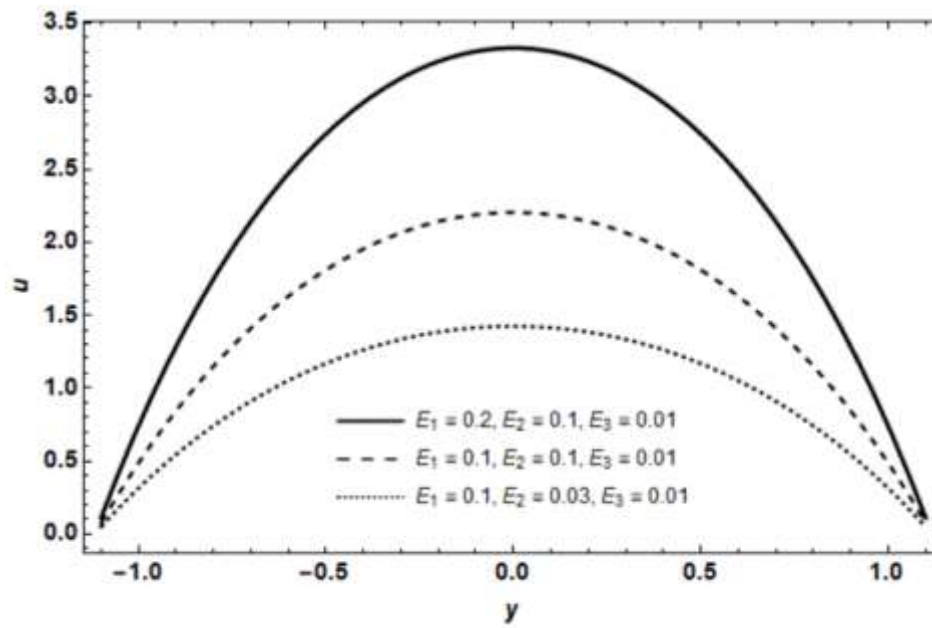
Figure 3.10 Variation of wall properties on velocity field
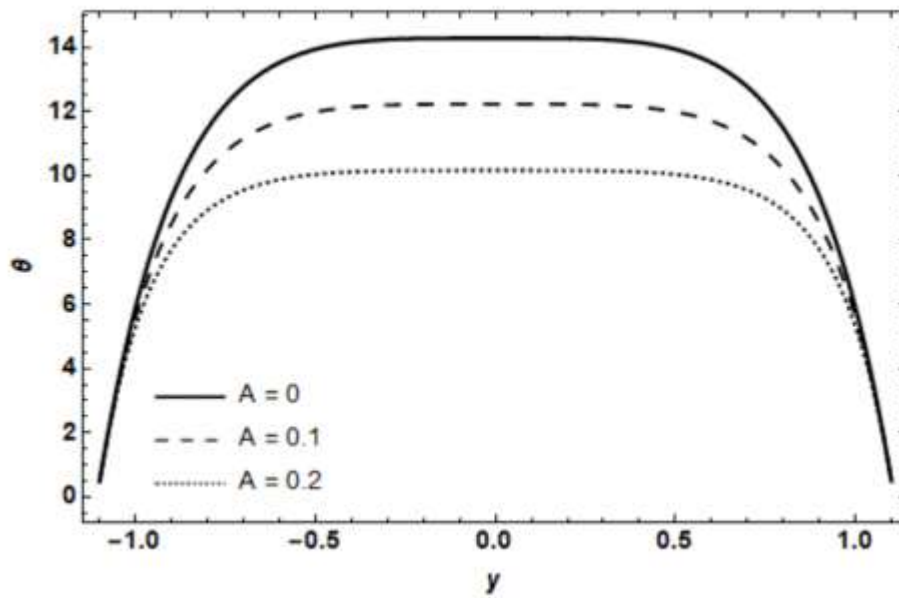
Figure 3.11 Variation of *A* on temperature field at *A= 0, 0.1, 0.2*
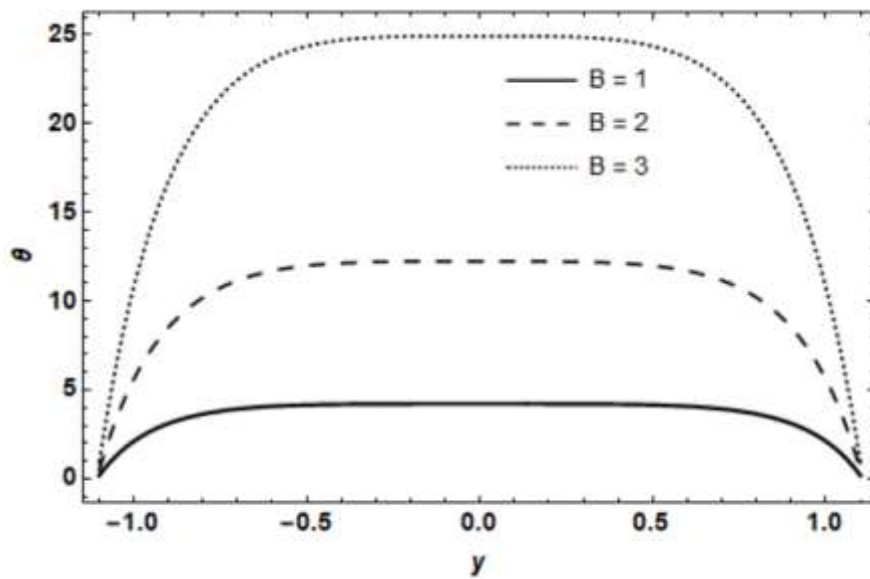
Figure 3.12 Fluctuations of *B* on temperature field at *B= 1, 2, 3*
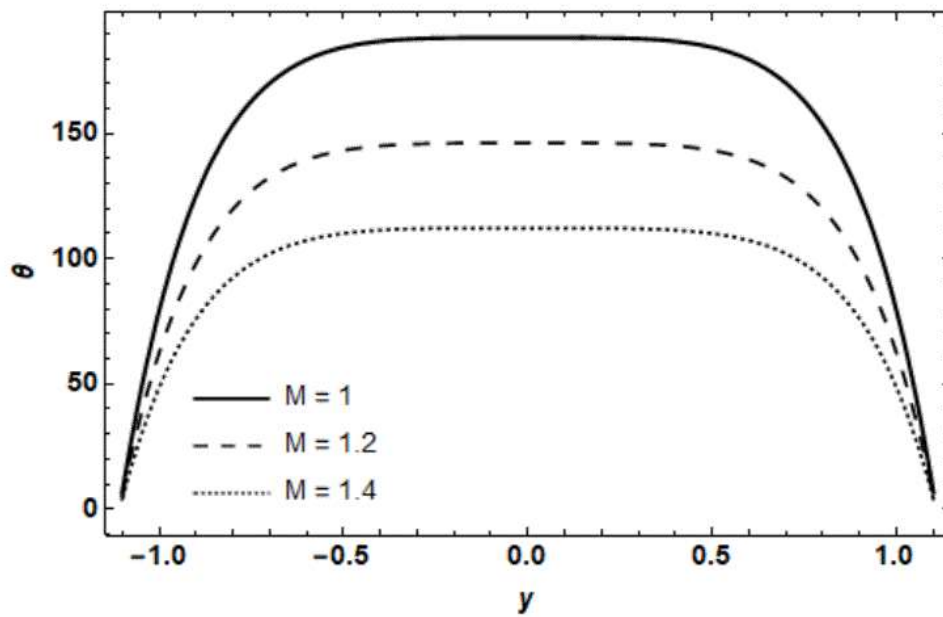
Figure 3.13 Fluctuations of *M* on temperature field at *M= 1, 1.2, 1.4*
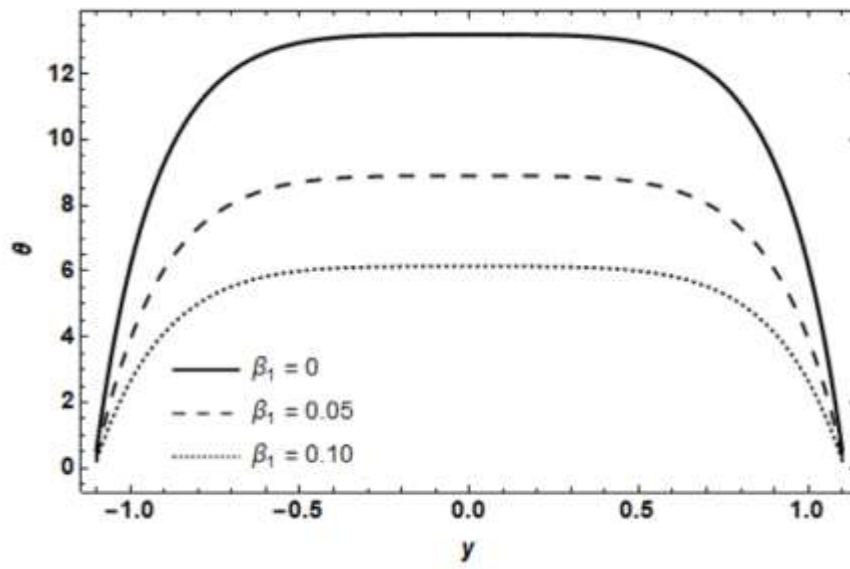
Figure 3.14 Fluctuations of β_1 on temperature field at $\beta_1 = 0, 0.05, 0.10$
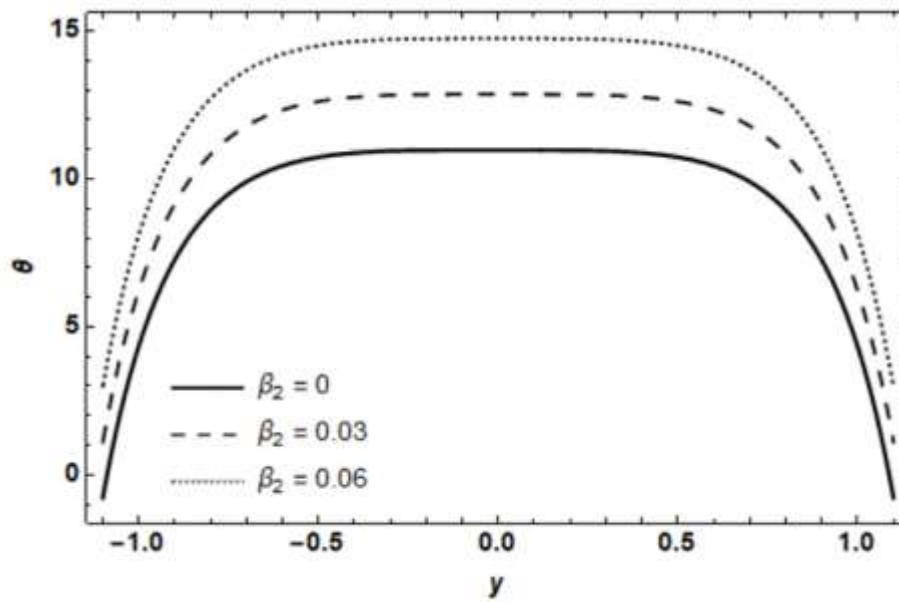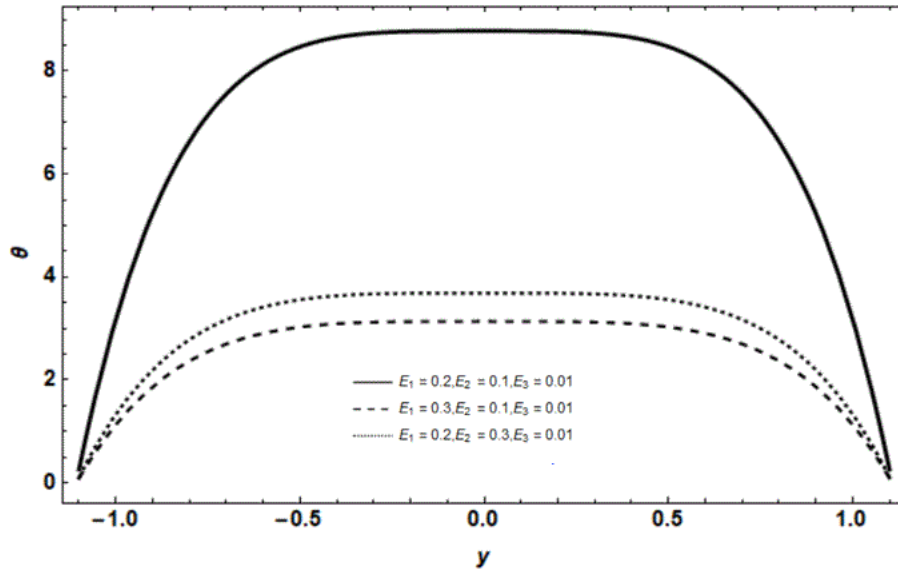

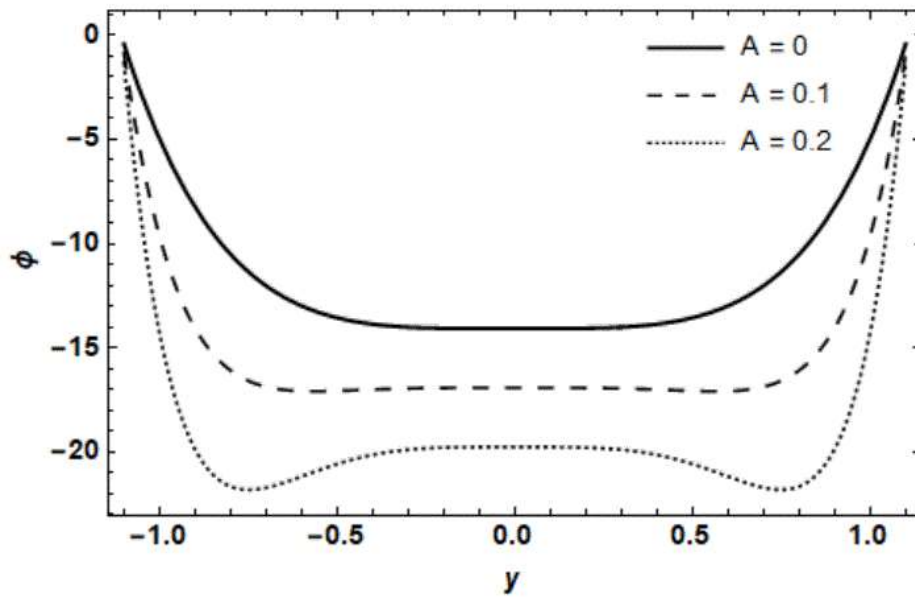**Figure 3.15** Variation of β_2 on temperature field at $\beta_2 = 0, 0.03, 0.06$
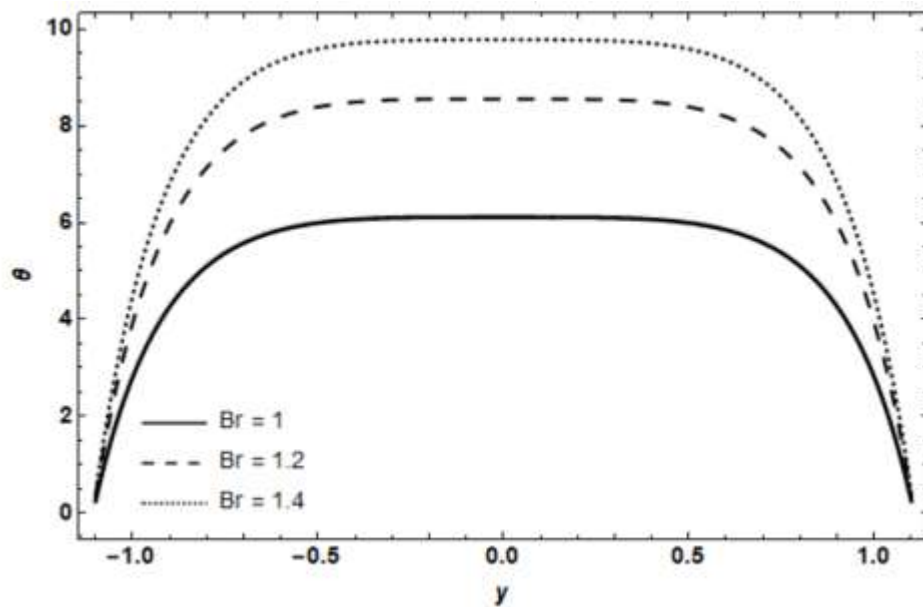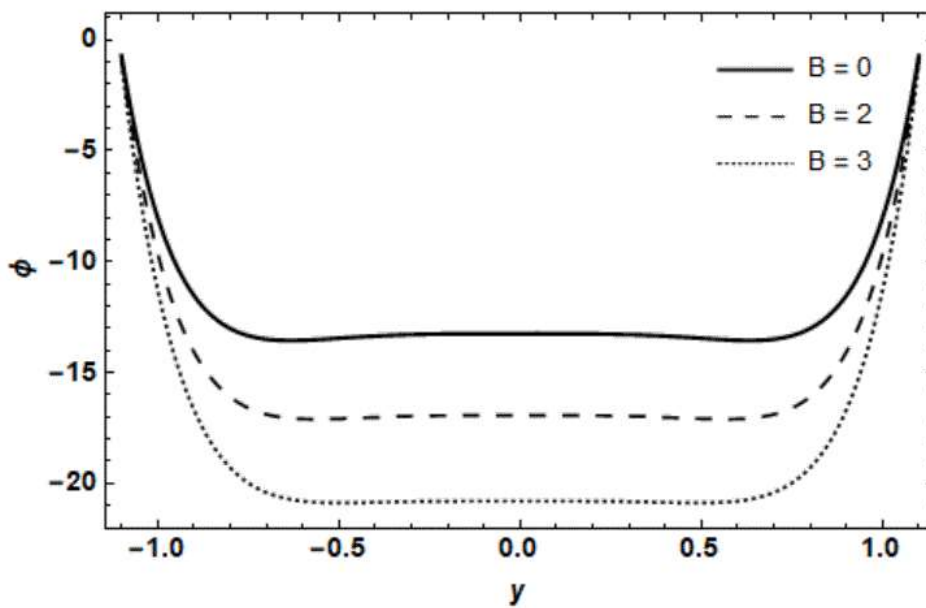
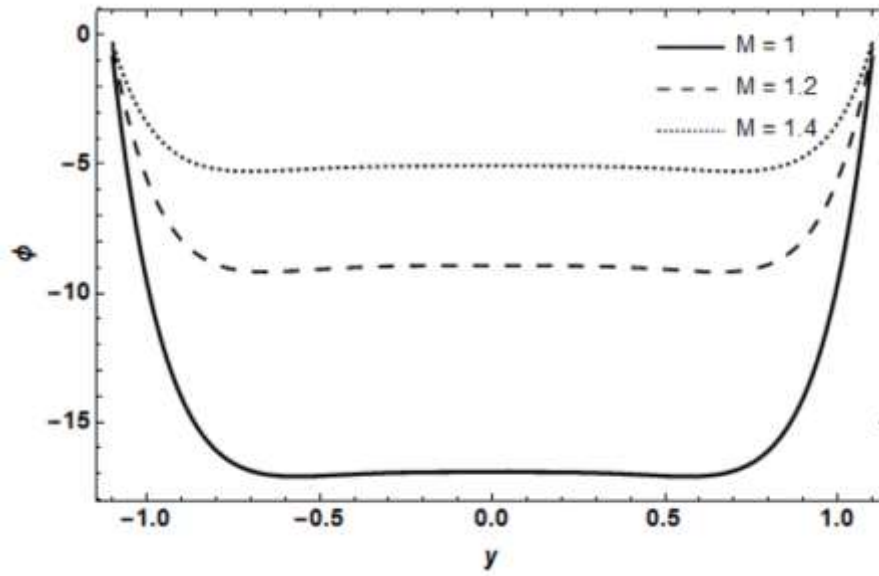**Figure 3.16** Fluctuations of *Br* on temperature field at *Br= 1, 1.2, 1.4*

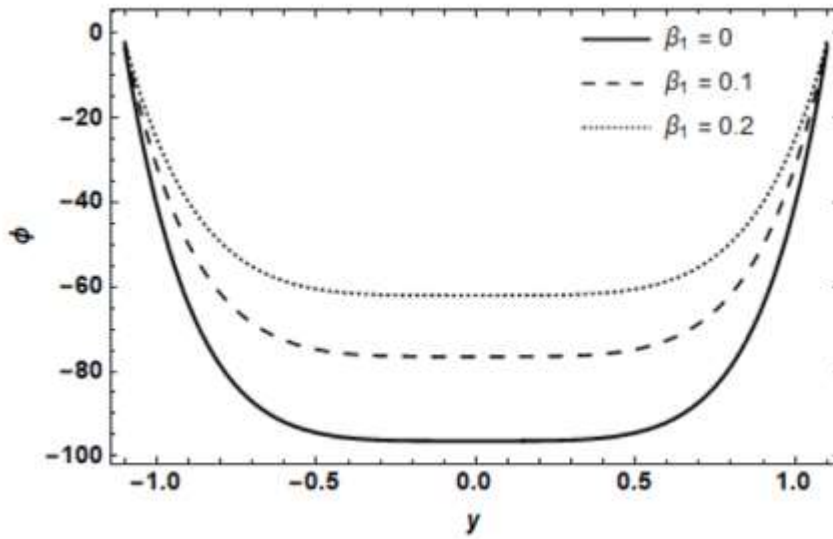**Figure 3.17** Variation of wall properties on profile of temperature

Figure 3.18 Variation of *A* on concentration field at *A= 0, 0.1, 0.2*

Figure 3.19 Variation of *B* on concentration profile at *B= 0, 2, 3*

Figure 3.20 Variation of *M* on concentration field at *M= 1, 1.2, 1.4*

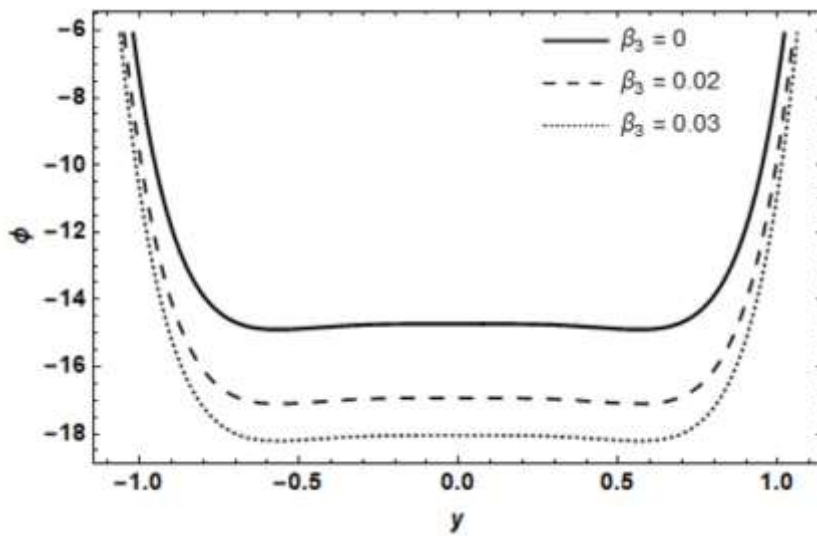**Figure 3.21** Variation of β_1 on concentration field at $\beta_1= 0, 0.1, 0.2$

Figure 3.22 Variation of β_3 on concentration field at β_3= 0, 0.02, 0.03
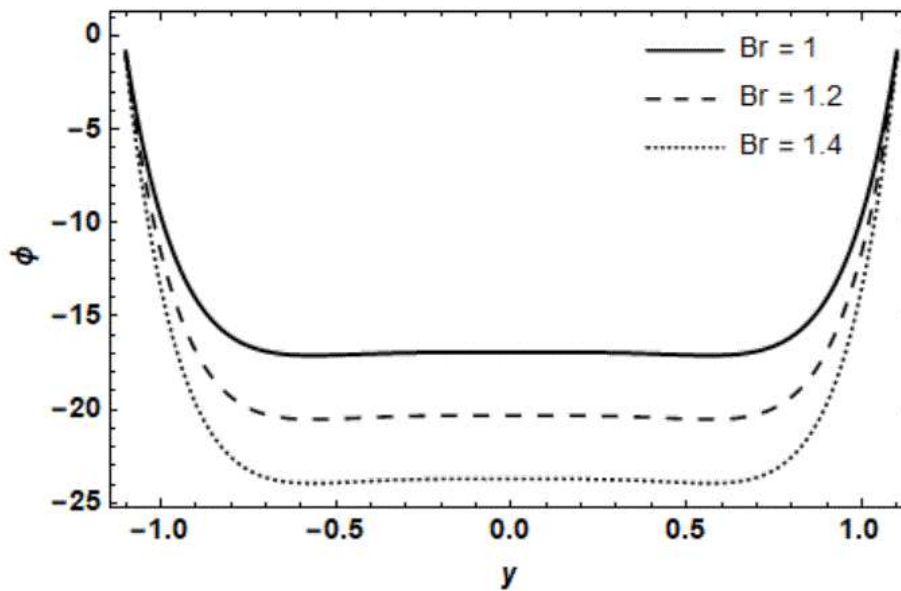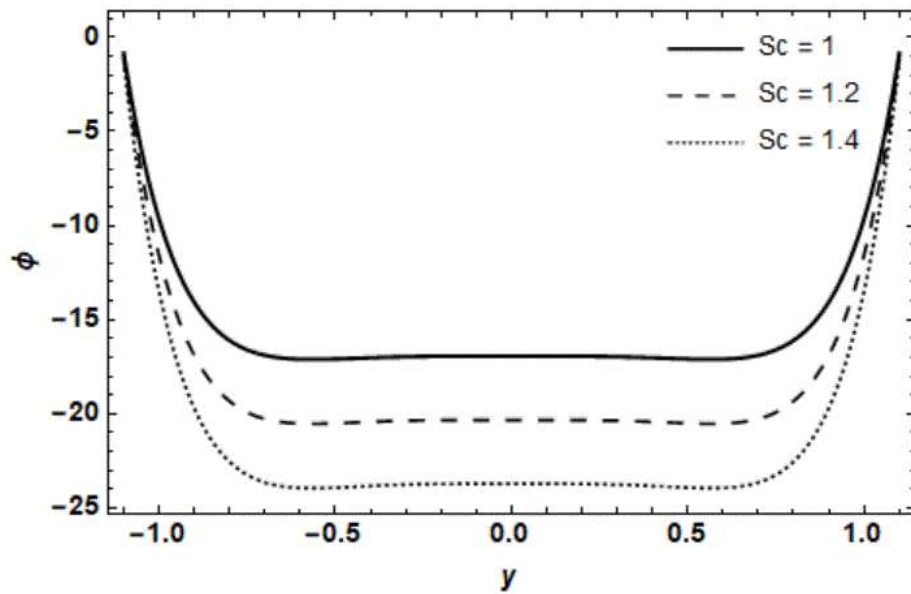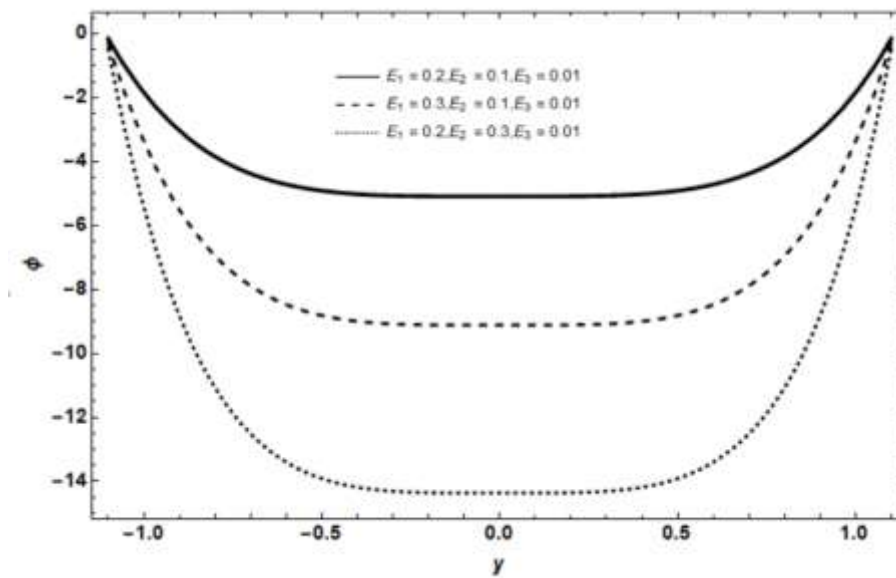

Figure 3.23 Variation of *Br* on concentration field at *Br= 1, 1.2, 1.4*

Figure 3.24 Variation of *Sc* on concentration file at *Sc= 1, 1.2, 1.4*

Figure 3.25 Variation of wall properties on concentration profile

3.5 Conclusion

By taking into account wall characteristics and heat/mass transfer, the slip effects on the magnetohydrodynamic (MHD) peristaltic flow of an Eyring-Powell fluid are examined. Viscous dissipation effects of considerable magnitude are taken into account in the mathematical formulation. The lubrication assumptions are used to generate a perturbation solution.Variations in embedded parameters, in particular those of the Eyring-Powell fluid, have a considerable impact on the flow fields. Comparing hydrodynamic flow to magnetohydrodynamic flow, it is found that the axial velocity in the former is higher. The flow is also accelerated in the axial direction when velocity slip is present. In order to improve heat transfer from the channel walls, viscous dissipation is quite important.

CHAPTER 4

Analysis of Peristaltic Eyring-Powell Fluid with an Inclined Magnetic Field in a Non-Uniform Porous Channel

4.1 Introduction

This system investigates the properties of the Eyring-Powell fluid's stable, laminer rheology from a peristaltic non-uniform inclined channel. A body force term of the momentum equation is used to simulate the magneto hydrodynamics (MHD) and porosity effects, while the rheological equations are stated in the Cartesian system. The form of the system of partial differential equations represents the projected model. Temperature and velocity profiles are used to visually represent the data. A comparative analysis with the published literature validates the current findings.
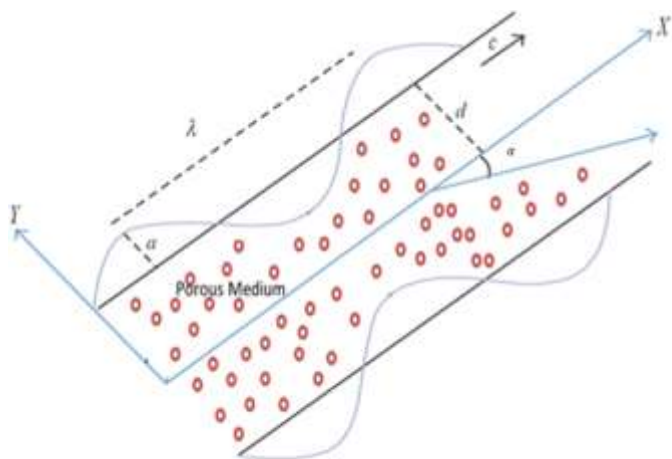
Figure 4.1 Geometry of Problem

4.2   Mathematical Formulation

This study examines how heat and mass transfer affect an Eyring-Powell fluid peristaltic flow in a two-dimensional, axisymmetric channel. The fluid is thought to drive electrically when a porous material and an angled magnetic field exist. Through the channel walls, the flow produces sinusoidal waves that propagate at a constant speed c. The wave shapes along the wall are given as

$$h(x,t) = b \sin\frac{2\pi}{\lambda}(x - ct) + d(x), \tag{4.1}$$

where

$$d(x) = mx + a, \qquad m \ll 1.$$

λ is the wavelength, wave amplitude is represented by b, t is the time, n is the dimensional parameter and a is the width.

The velocity pattern of peristaltic flow is

$$\mathbf{V} = [u(x,y), v(x,y)] \tag{4.2}$$

The equations of continuity, momentum and energy are as follows

$$\nabla.\mathbf{V} = 0, \tag{4.3}$$

$$\rho\frac{d\mathbf{V}}{dt} = div\boldsymbol{\tau} + \rho\mathbf{b}, \tag{4.4}$$

$$\rho C_p\frac{dT}{dt} = -div\mathbf{q} + \boldsymbol{\tau}.\mathbf{L}, \tag{4.5}$$

where

$$\mathbf{q} = -\mathbf{k}gradT,$$

and the body forces under consideration are:

$$\rho\mathbf{b} = -\sigma\beta_0^2\mathbf{V} - \frac{\mu}{k}\mathbf{V},$$

with same tensor as given in chapter 3 from equations (3.2) to (3.10).

The Eyring-Powell fluid model's governing equations are provided as:

$$\frac{\partial u}{\partial x} + \frac{\partial v}{\partial y} = 0,$$

(4.6)

The x-component of the momentum equation is as under:

$$\rho\left(\frac{\partial u}{\partial t} + u\frac{\partial u}{\partial x} + v\frac{\partial u}{\partial y}\right) = -\frac{\partial p}{\partial x} + \left(\mu + \frac{1}{\beta c_1}\right)\left(\frac{\partial^2 u}{\partial x^2} + \frac{\partial^2 u}{\partial y^2}\right)$$

$$-\frac{1}{3\beta c_1^3}\frac{\partial}{\partial x}\left[\left\{\left(\frac{\partial u}{\partial y} + \frac{\partial v}{\partial x}\right)^2 + 2\left(\frac{\partial v}{\partial y}\right)^2 + 2\left(\frac{\partial u}{\partial x}\right)^2\right\}\frac{\partial u}{\partial x}\right]$$

$$-\frac{1}{6\beta c_1^3}\frac{\partial}{\partial y}\left[\left\{2\left(\frac{\partial u}{\partial x}\right)^2 + \left(\frac{\partial u}{\partial y} + \frac{\partial v}{\partial x}\right)^2 + 2\left(\frac{\partial v}{\partial y}\right)^2\right\}\left(\frac{\partial u}{\partial y} + \frac{\partial v}{\partial x}\right)\right]$$

$$+\rho g \sin\alpha - \sigma\beta_0^2 \cos\beta(u\cos\beta - v\sin\beta) - \frac{\mu}{K}u,$$

(4.7)

The y-component of the momentum equation is given as:

$$\rho\left(\frac{\partial v}{\partial t} + u\frac{\partial v}{\partial x} + v\frac{\partial v}{\partial y}\right) = -\frac{\partial p}{\partial y} + \left(\mu + \frac{1}{\beta c_1}\right)\left(\frac{\partial^2 v}{\partial x^2} + \frac{\partial^2 v}{\partial y^2}\right)$$

$$-\frac{1}{3\beta c_1^3}\frac{\partial}{\partial y}\left[\left\{\left(\frac{\partial u}{\partial y} + \frac{\partial v}{\partial x}\right)^2 + 2\left(\frac{\partial u}{\partial x}\right)^2 + 2\left(\frac{\partial v}{\partial y}\right)^2\right\}\frac{\partial v}{\partial x}\right]$$

$$-\frac{1}{6\beta c_1^3}\frac{\partial}{\partial y}\left[\left\{2\left(\frac{\partial u}{\partial x}\right)^2 + \left(\frac{\partial u}{\partial y} + \frac{\partial v}{\partial x}\right)^2 + 2\left(\frac{\partial v}{\partial y}\right)^2\right\}\left(\frac{\partial u}{\partial y} + \frac{\partial v}{\partial x}\right)\right]$$

$$+\rho g \cos\alpha - \sigma\beta_0^2 \sin\beta(u\cos\beta - v\sin\beta) - \frac{\mu}{K}v,$$

(4.8)

The energy equation is given as below:

$$\rho C_p\left(\frac{\partial T}{\partial t} + u\frac{\partial T}{\partial x} + v\frac{\partial T}{\partial y}\right) = k\left(\frac{\partial^2 T}{\partial x^2} + \frac{\partial^2 T}{\partial y^2}\right) + \left(\mu + \frac{1}{\beta c_1}\right)\left[4\left(\frac{\partial u}{\partial x}\right)^2 + \left(\frac{\partial u}{\partial y} + \frac{\partial v}{\partial x}\right)^2\right] -$$

$$\frac{2}{3\beta c_1^3}\left(\frac{\partial u}{\partial x}\right)^2\left\{2\left(\frac{\partial v}{\partial y}\right)^2 + 2\left(\frac{\partial u}{\partial x}\right)^2 + \left(\frac{\partial u}{\partial y} + \frac{\partial v}{\partial x}\right)^2\right\}$$

$$-\frac{1}{6\beta c_1^3}\left(\frac{\partial u}{\partial y} + \frac{\partial v}{\partial x}\right)^2\left\{2\left(\frac{\partial u}{\partial x}\right)^2 + \left(\frac{\partial u}{\partial y} + \frac{\partial v}{\partial x}\right)^2 + 2\left(\frac{\partial v}{\partial y}\right)^2\right\},$$

(4.9)

Here p be the pressure, applied magnetic field is represented by β_0, σ is the electrical conductivity of fluid.

The following are the Boundary Conditions:

$$\frac{\partial}{\partial x}\left(\tau\frac{\partial^2}{\partial x^{*2}} + m\frac{\partial^2}{\partial t^{*2}} + d\frac{\partial}{\partial t}\right)h = \left(\mu + \frac{1}{\beta c_1}\right)\left(\frac{\partial^2 u}{\partial x^{*2}} + \frac{\partial^2 u}{\partial y^{*2}}\right) - \rho\left(\frac{\partial u}{\partial t} + u\frac{\partial u}{\partial x} + v\frac{\partial u}{\partial y^*}\right) - \frac{1}{6\beta c_1^3}\frac{\partial}{\partial y^*}\left[\left\{2\left(\frac{\partial u}{\partial x^*}\right)^2 + \right.\right.$$

$$\left. 2\left(\frac{\partial v}{\partial y^*}\right)^2 + \left(\frac{\partial u}{\partial y^*} + \frac{\partial v}{\partial x^*}\right)^2\right\}\left(\frac{\partial u}{\partial y^*} + \frac{\partial v}{\partial x^*}\right)\right] - \frac{1}{3\beta c_1^3}\frac{\partial}{\partial x^*}\left[\left\{2\left(\frac{\partial u}{\partial x^*}\right)^2 + 2\left(\frac{\partial v}{\partial y^*}\right)^2 + \left(\frac{\partial u}{\partial y^*} + \frac{\partial v}{\partial x^*}\right)^2\right\}\frac{\partial u}{\partial x^*}\right] -$$

$$\rho g \sin\alpha - \sigma\beta_0^2\cos\beta(u\cos\beta - v\sin\beta)\frac{\mu}{K}u, \qquad\qquad at \quad y{=}h, \qquad\qquad (4.10)$$

$$u = 0, \qquad T = T_1, \qquad\qquad at \ y = h, \qquad\qquad (4.11)$$

$$\frac{\partial u}{\partial y} = 0, \qquad \frac{\partial T}{\partial y} = T_0, \qquad\qquad at \ y = 0, \qquad\qquad (4.12)$$

where the variables T_0 and T_1 represent the temperature at the lower and higher walls, d represents the wall damping coefficient, m be the mass of the plate per unit area, and τ stands for elastic strain.

The stream function ψ is now introduced as:

$$u = \frac{\partial\psi}{\partial y}, \qquad v = -\frac{\partial\psi}{\partial x}. \qquad\qquad (4.13)$$

The dimensionless quantities are:

$$x' = \frac{x}{\lambda}, y' = \frac{y}{d_1}, \psi' = \frac{\psi}{cd_1}, t' = \frac{ct}{\lambda}, p' = \frac{pd_1^2}{c\lambda\mu}, B = \frac{1}{\mu\beta c_1}, A = \frac{Bc^2}{2d_1^2 c_1^2},$$

$$\delta = \frac{d_1}{\lambda}, \theta = \frac{T - T_0}{T_0}, Re = \frac{\rho cd_1}{\mu}, M^2 = \sqrt{\frac{\sigma}{\mu}}\beta_0 d_1, Pr = \frac{\mu C_P}{\kappa}, Ec = \frac{c^2}{C_p T_0},$$

$$k = \frac{K}{d_1^2}, F = \frac{cv}{gd_1^2}, E_1 = -\tau\frac{d_1^3}{\lambda^3\mu c}, E_2 = \frac{mcd_1^3}{\lambda^3\mu}, E_3 = \frac{dd_1^3}{\lambda^2\mu} \qquad\qquad (4.14)$$

In previously indicated values A and B are the material variables for the Eyring-Powell fluid model, Pr the Prandtl number, δ the wave number, Re the Reynolds number, Ec the Eckert number, θ the temperature distribution, mass per unit area parameter E_2, wall elastance

parameter E_1 and wall damping value E_3.

    After applying the lubrication assumptions, creating the stream function, which automatically solves the continuity equation, and non-dimensionalization, problem is reduced as:

$$\frac{\partial p'}{\partial x'} = (1+B)\frac{\partial^3 \psi'}{\partial y'^3} - \frac{A}{3}\frac{\partial}{\partial y'}\left(\frac{\partial^2 \psi'}{\partial y'^2}\right)^3 - (M\cos\beta)^2 \frac{\partial \psi'}{\partial y'} - \frac{1}{k}\frac{\partial \psi'}{\partial y'} + \frac{\sin\alpha}{F}, \tag{4.15}$$

$$\frac{\partial p'}{\partial y'} = 0, \tag{4.16}$$

$$\frac{1}{Pr}\frac{\partial^2 \theta}{\partial y^2} + Ec(\frac{\partial^2 \psi'}{\partial y'^2})^2\left[(1+B) - \frac{A}{3}\left(\frac{\partial^2 \psi'}{\partial y'^2}\right)^2\right] = 0, \tag{4.17}$$

and the boundary conditions become:

$$\frac{\partial}{\partial x}\left(E_1 \frac{\partial^2}{\partial x'^2} + E_2 \frac{\partial^2}{\partial t'^2} + E_3 \frac{\partial}{\partial t'}\right)h = (1+B)\frac{\partial^3 \psi'}{\partial y'^3} - \frac{A}{3}\frac{\partial}{\partial y'}\left(\frac{\partial^2 \psi'}{\partial y'^2}\right)^3$$

$$-(M\cos\beta)^2 \frac{\partial \psi'}{\partial y'} - \frac{1}{k}\frac{\partial \psi'}{\partial y'}, \qquad at\ y' = h \tag{4.18}$$

$$\frac{\partial \psi'}{\partial y'} = 0, \qquad \theta = 1, \qquad at\ y' = h \tag{4.19}$$

$$\psi' = 0, \quad \frac{\partial^2 \psi'}{\partial y'^2} = 0, \qquad \frac{\partial \theta}{\partial y'} = 0, \qquad at\ y' = 0 \tag{4.20}$$

Combining (4.15) and (4.16), compatibility equation takes the form

$$(1+B)\frac{\partial^4 \psi'}{\partial y'^4} - \frac{A}{3}\frac{\partial^2}{\partial y'^2}\left(\frac{\partial^2 \psi'}{\partial y'^2}\right)^3 - N_1{}^2 \frac{\partial^2 \psi'}{\partial y'^2} = 0, \tag{4.21}$$

where

$$N_1 = M^2 \cos^2\beta + \frac{1}{k}.$$

4.3   Method of Solution

    Due to the involvement of small parameter 'A' in the governing equations, To solve the system concerning the small Eyring-Powell fluid perimeter A, we can use the perturbation technique.

$$\psi' = \psi'_0 + A\psi'_1 + O(A)^2, \tag{4.22}$$

$$\theta' = \theta'_0 + A\theta'_1 + O(A)^2. \tag{4.23}$$

4.3.1 Zeroth –Order System

The form of the zeroth order system is

$$(1+B)\frac{\partial^4 \psi'_0}{\partial y'^4} - N_1{}^2 \frac{\partial^2 \psi'_0}{\partial y'^2} = 0, \tag{4.24}$$

$$\frac{\partial^2 \theta'_0}{\partial y'^2} + Br(1+B)\left(\frac{\partial^2 \psi'_0}{\partial y'^2}\right)^2 = 0, \tag{4.25}$$

and the boundary conditions are

$$\frac{\partial}{\partial x}\left(E_1 \frac{\partial^2}{\partial x'^2} + E_2 \frac{\partial^2}{\partial t'^2} + E_3 \frac{\partial}{\partial t'}\right)h = (1+B)\frac{\partial^3 \psi'_0}{\partial y^{*3}} - N_1{}^2 \frac{\partial \psi'_0}{\partial y^*}, \qquad at \quad y' = h \tag{4.26}$$

$$\psi'_0 = 0, \qquad \frac{\partial^2 \psi'_0}{\partial y'^2} = 0, \qquad \frac{\partial \theta'_0}{\partial y'} = 0, \qquad at \; y' = 0, \tag{4.27}$$

$$\theta'_0 = 1, \qquad \frac{\partial \psi'_0}{\partial y'} = 0, \qquad at \; y' = h. \tag{4.28}$$

4.3.2 First order system:

The first order system is of the form

$$(1+B)\frac{\partial^4 \psi'_1}{\partial y'^4} - \frac{1}{3}\frac{\partial^2}{\partial y'^2}\left(\frac{\partial^2 \psi'_0}{\partial y'^2}\right)^3 - N_1{}^2 \frac{\partial^2 \psi'_1}{\partial y'^2} = 0, \tag{4.29}$$

$$\frac{\partial^2 \theta'_1}{\partial y'^2} + 2Br(1+B)\left(\frac{\partial^2 \psi'_0}{\partial y'^2}\right)\left(\frac{\partial^2 \psi'_1}{\partial y'^2}\right) - \frac{Br}{3}\left(\frac{\partial^2 \psi'_0}{\partial y'^2}\right)^4 = 0, \tag{4.30}$$

and the boundary conditions are

$$(1+B)\frac{\partial^3 \psi'_1}{\partial y'^3} - \frac{1}{3}\frac{\partial}{\partial y'}\left(\frac{\partial^2 \psi'_0}{\partial y'^2}\right)^3 - N_1{}^2 \frac{\partial^2 \psi'_1}{\partial y'^2} = 0 \quad at \; y' = h, \tag{4.31}$$

$$\psi'_1 = 0, \qquad \frac{\partial^2 \psi'_1}{\partial y'^2} = 0, \qquad \frac{\partial \theta'_1}{\partial y'} = 0, \qquad at \; y' = 0, \tag{4.32}$$

$$\frac{\partial \psi'_1}{\partial y'} = 0, \qquad \theta'_1 = 0 \qquad at \; y' = h. \tag{4.33}$$

4.4   Results and Discussion

The behavior of the parameters used in the axial velocity (u), temperature (θ), pressure and streamlines expressions is explained in this section. In particular, inclination of magnetic field (β), Brinkman number *(Br)*, and Magnetic parameter (M), non-uniform term (m), porosity parameter (k) are examined. To examine the effects of these settings, graphs were made using the MATHEMATICA programming language.

Trapping is one of the most significant phenomena in peristaltic movement. The formation of a circulating bolus caused by streamlines splitting under specific circumstances is referred to as trapping. The trapped bolus travels at the same speed as the wave because it is completely encircled by the peristaltic waves. In Figure 4.2(a) and (b) the influence of Eyring-Powell fluid parameter A is portrayed. The size of the confined bolus and the number of streamlines both decrease as A rises. The impact of Eyring-Powell fluid parameter B on the streamline patterns can be seen in Figures 4.3(a) and 4.3(b). It can be seen that increasing B both the number of circulations and the size of the trapped bolus decreases.

Figure 4.4(a) and (b) show that by increasing the value of magnetic parameter, bolus size and number of circulations decreases. Figure 4.5(a) and (b) shows the same behavior when the value of porosity parameter increases. From figures 4.6(a) and (b) we conclude that by increasing the value of β, the volume of the trapped bolus increases. The impact of wall properties is given in figure 4.7(a)-(b), by enhancing the values of the wall properties, there is a decrease in the size of trapped bolus.

Velocity field is the most noticeable feature of fluids flow. Firstly analytical solution for velocity is calculated, and then other flow variables are determined. It is shown in figure 4.8 that by increasing the value of A the velocity profile decreases. Figure 4.9 demonstrates how the fluid's velocity decreases when the Eyring-Powell fluid parameter B value rises. Figure 4.10 depicts that rise in the value of M shows reduction in the velocity because with the increase in the value of M resistive force increases. Figure 4.11 show that there is a decrease in flow resistance and an increase in fluid velocity within the channel as the porosity of the walls increases. It is seen from figure 4.12 that velocity profile increases with rise in inclination angle β because magnetic field's inclination can change the Lorentz force, lessen magnetic drag, and produce secondary flow patterns, all of which increase fluid velocity. Figure 4.13 show that as m increases, velocity increases because when we increase non-uniformity, then the regions experiences lower viscosity leading to an increase in overall velocity. Effects of wall properties on axial velocity is sketched in figure 4.14. It reveals that the flow in the axial direction is accelerated by increases in wall elasticityE_1, wall damping parameter E_3 ,wall mass per unit area E_2.

Figure 4.15 to 4.22 show the significance of different emerging flow characteristics on the fluid's temperature θ. Figure 4.15 shows that as the value of parameter A increase, temperature decreases. Figure 4.16 display the trend of temperature profile when the fluid parameter B is increased. Figure 4.17 demonstrates that reduction in temperature profile as increase in value of magnetic parameter. Figure 4.18 depicts that the rise in inclination angle β also gives an increase in temperature profile. It is seen in figure 4.19 that as porosity of walls increases temperature increases because thermal conductivity reduces and surface area for heat exchange increases. Figure 4.20 depicts that as m increase, there is an increase in temperature distribution. As the value of Brinkman number increases temperature increases because when viscous dissipation enhances, there is a larger energy conversion from kinetic to thermal energy, which raises fluid temperature as shown in figure 4.21. Figure 4.22 shows that the fluid's temperature decreases as a result of a steady increase in wall mass per unit area E_2, wall elasticity E_1, or wall damping parameter E_3.
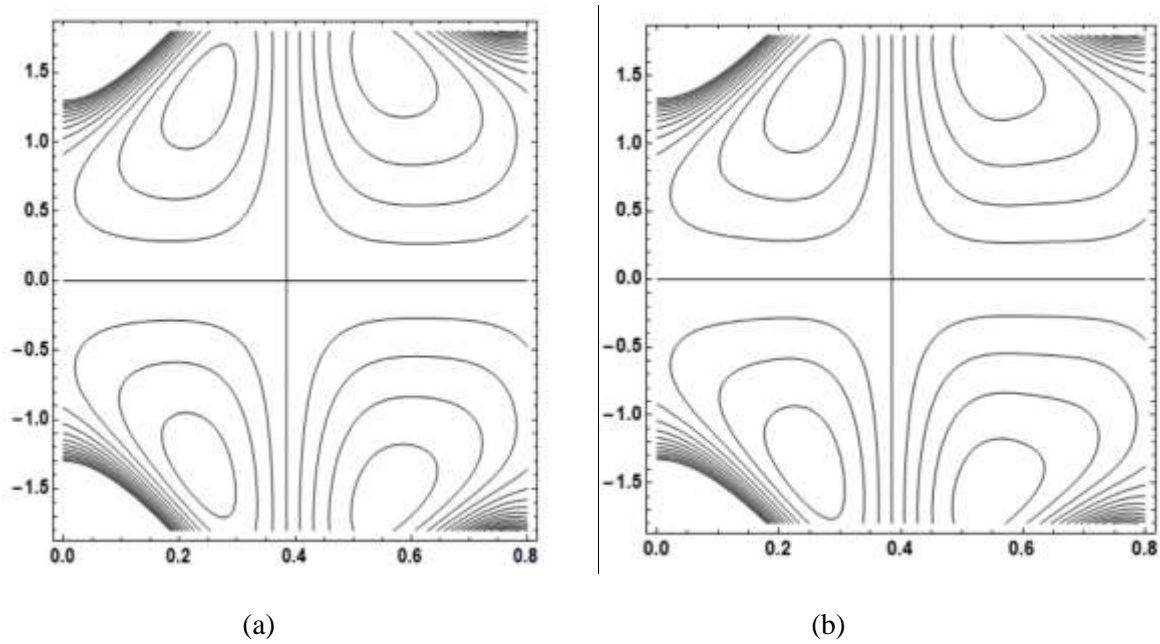
(a)

(b)
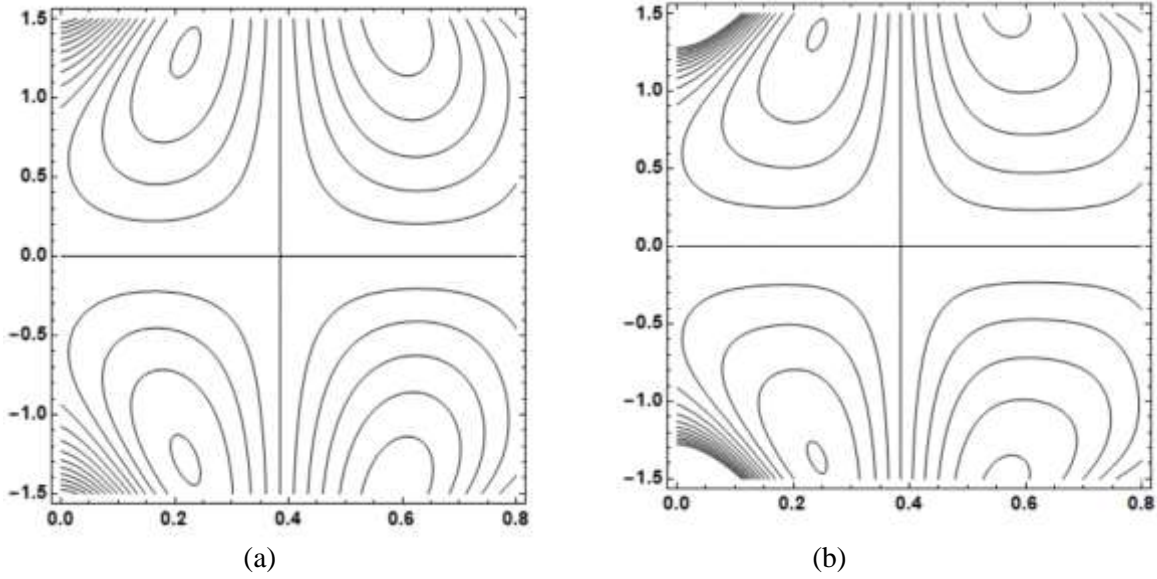
Figure 4.2 Effect of *A* on contours as E_1=0.1, E_2=0.2, E_3=0.3, $\epsilon =$ 0.5, t=0.16, B=2, M=2, β =0.01, k= 1.25, x=0.2, m =0.5 (a) A=0, (b) A=0.1

(a)

(b)
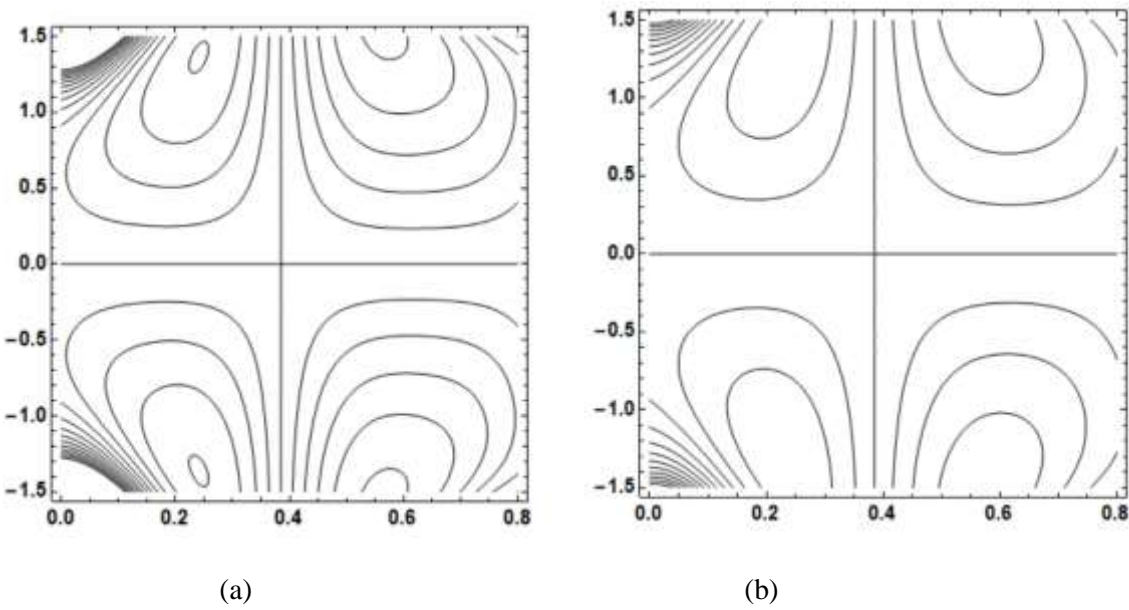
Figure 4.3 Effect of *B* on contours as $E_1 = 0.1$ E_2= 0.2, E_3= 0.3, $\epsilon = 0.5$, $t = 0.16$, A = 0.01, B = 2, M = 2, β = 0.01, k= 1.25, m =0.5 (a) B = 2 (b) B = 3.
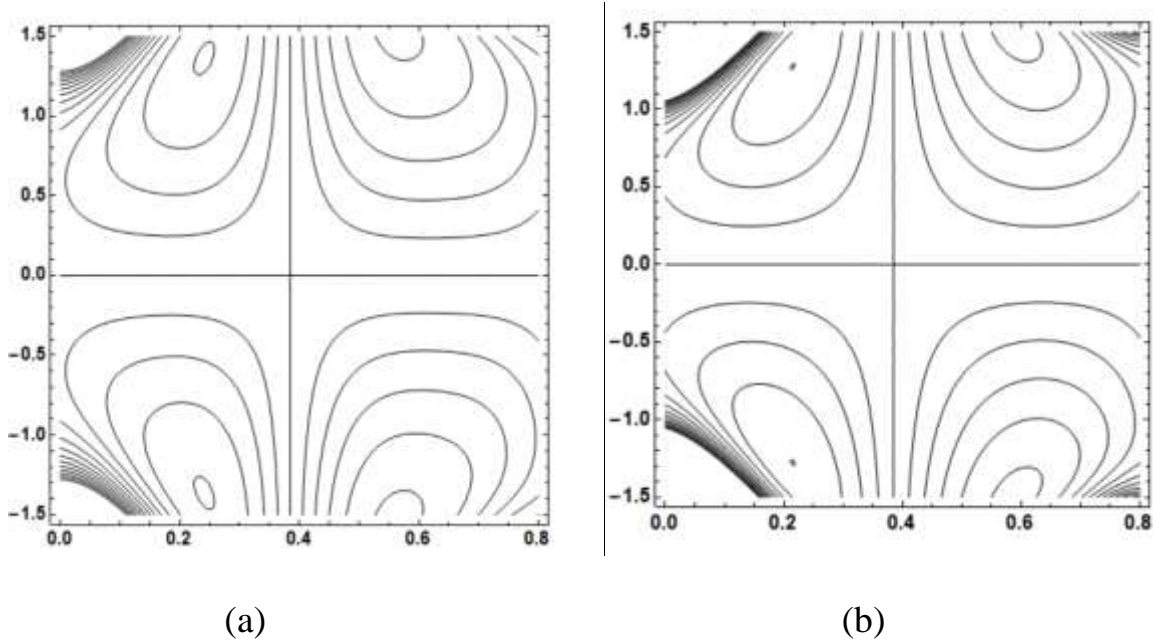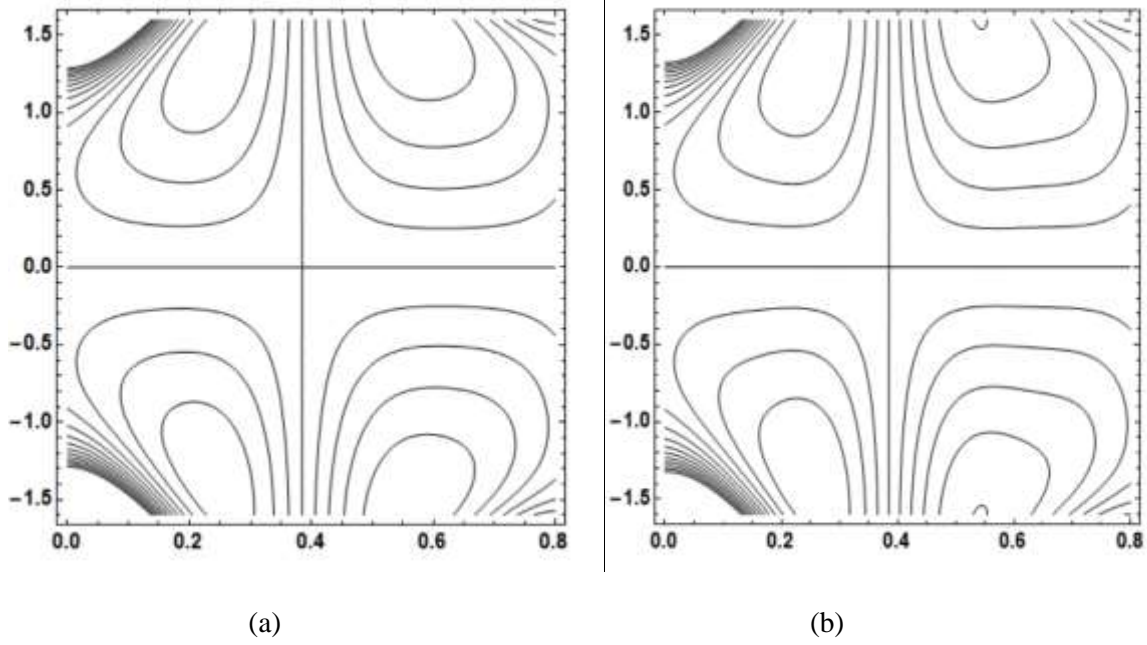
Figure 4.4 Effect of *M* on contours as $E_1 = 0.1$, $E_2 = 0.2$, $E_3 = 0.3$, $\epsilon = 0.5$, $t = 0.16$, $A = 0.01$, $B = 2$, $\beta = 0.01$, $k= 1.25$, $m =0.5$, $x=0.2$ (a) $M = 2$, (b) $M = 3$.
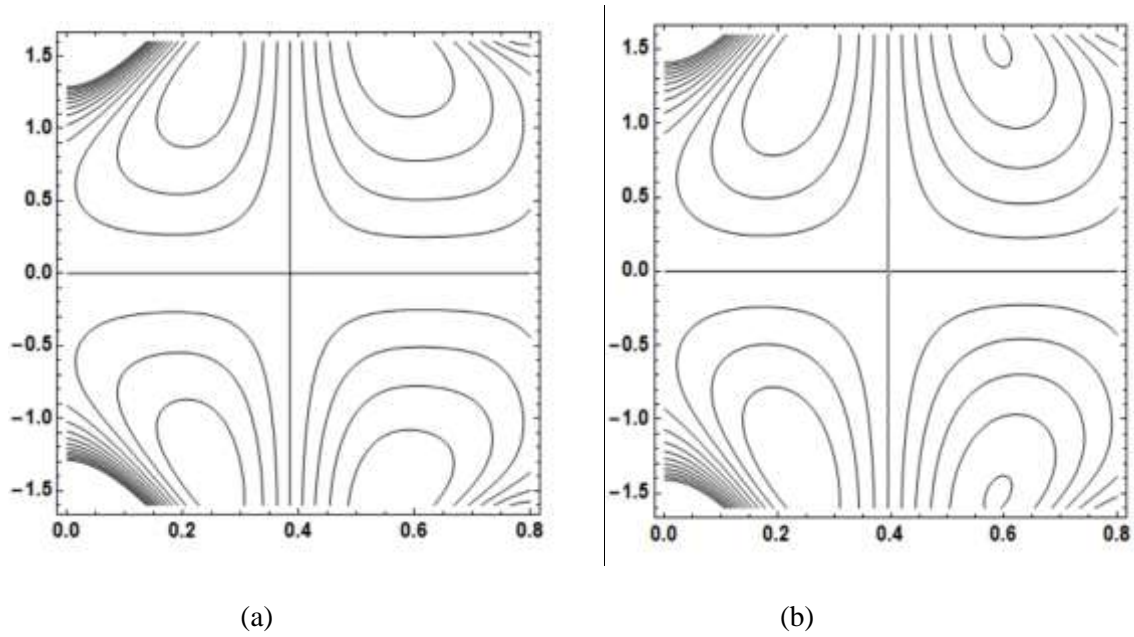

Figure 4.5 Effect of *k* on streamlines when $E_1 = 0.1$, $E_2 = 0.2$, $E_3 = 0.3$, $\epsilon = 0.5$, $t = 0.16$, $B = 2$, $A = 0.01$, $\beta = 0.01$, $M= 2$, $m =0.5$, $x=0.2$ (a) $k = 1.25$, (b) $k = 3.5$.

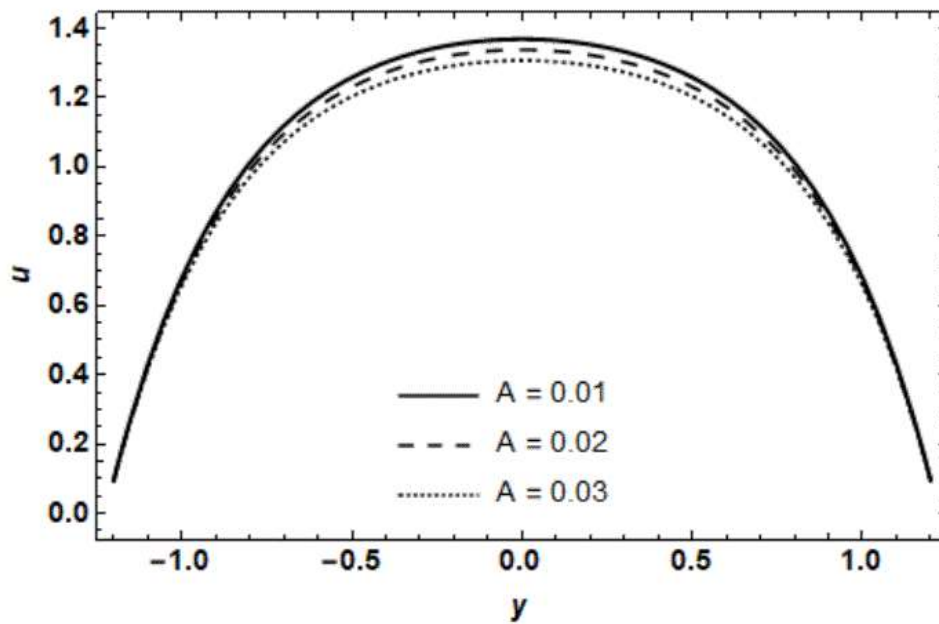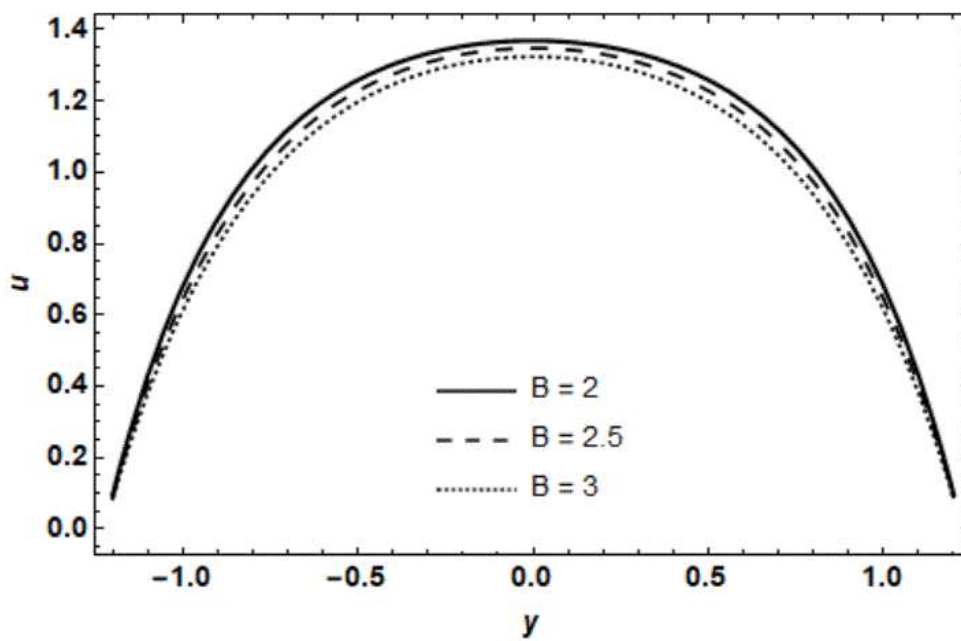(a)   (b)

Figure 4.6 Effects of β on contours as $E_1 = 0.1$, $E_2 = 0.2$, $E_3 = 0.3$, $\epsilon = 0.5$, $t = 0.16$, $A = 0.01$, $B = 2$, $M = 2$, $k= 1.25$, $x=0.2$, $m =0.5$, (a) β = 0.01, (b) β = 0.4.

(a)   (b)

Figure 4.7 Effect of wall properties on contours as $\epsilon = 0.5$, $t = 0.16$, $B = 2$, $A = 0.1$, $M = 2$, β = 0.01, 1.25, $m =0.5$, (a) $E_1 = 0.1$, $E_2 = 0.2$, $E_3 = 0.3$, (b) $E_1 = 0.2$, $E_2 = 0.3$, $E_3 = 0.3$.

Figure 4.8 Effect of Eyring-Powell fluid parameter on velocity field

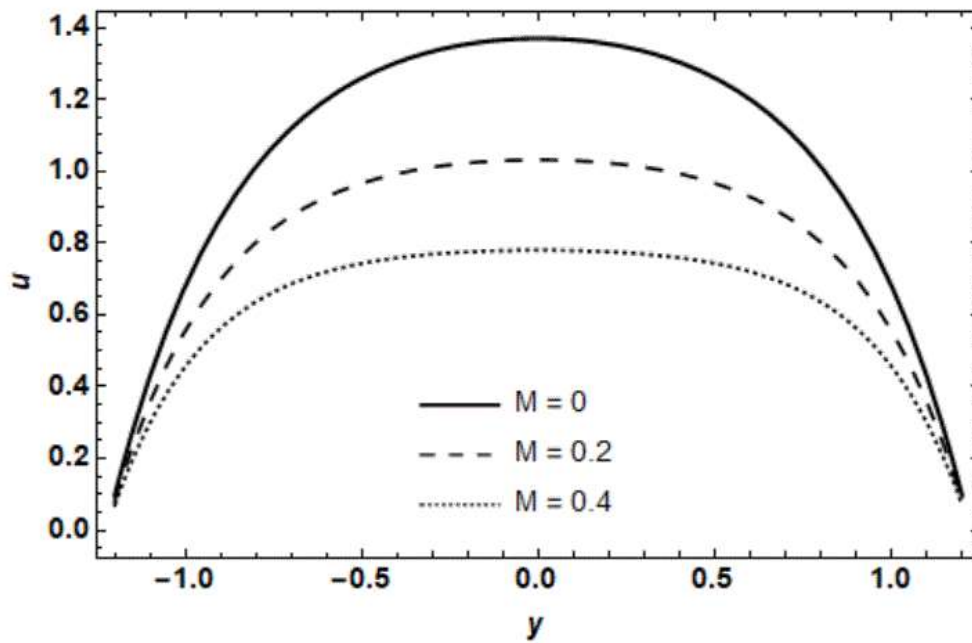**Figure 4.9** Effect of Eyring-Powell fluid parameter on velocity field.

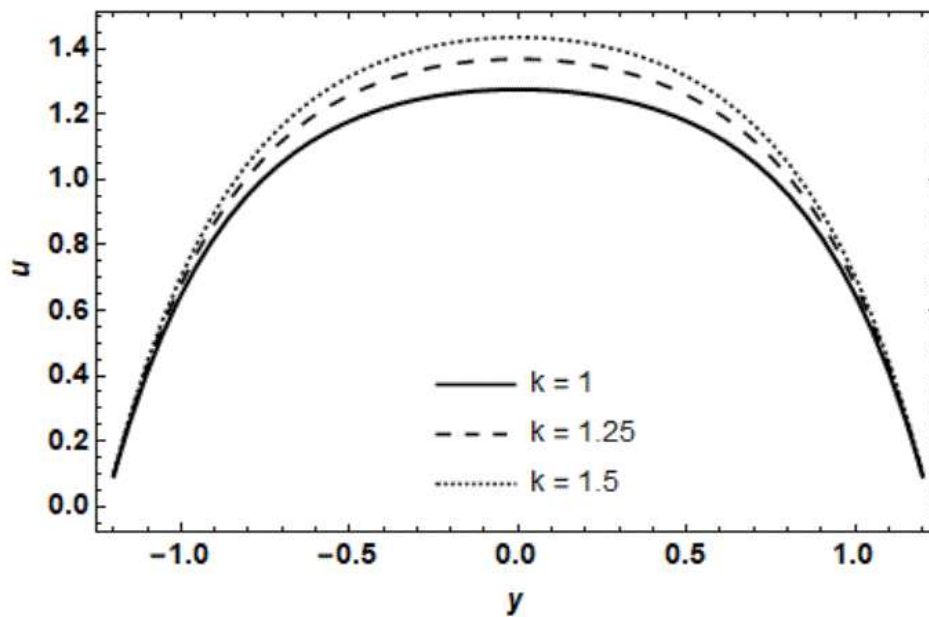**Figure 4.10** Effect of magnetic parameter on velocity field.

Figure 4.11 Effect of porosity parameter on velocity field.
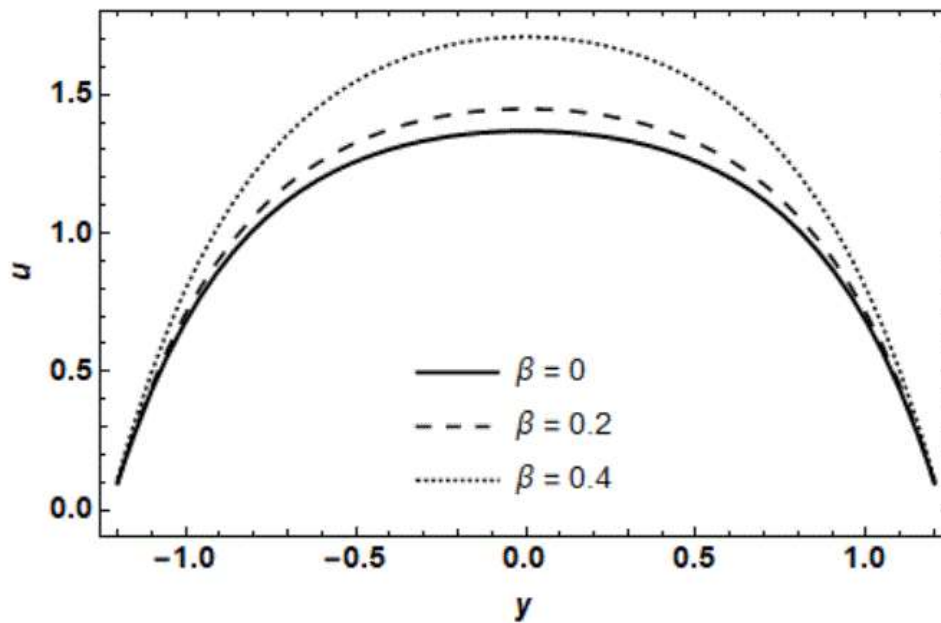
Figure 4.12 Effect of inclined parameter on velocity field.
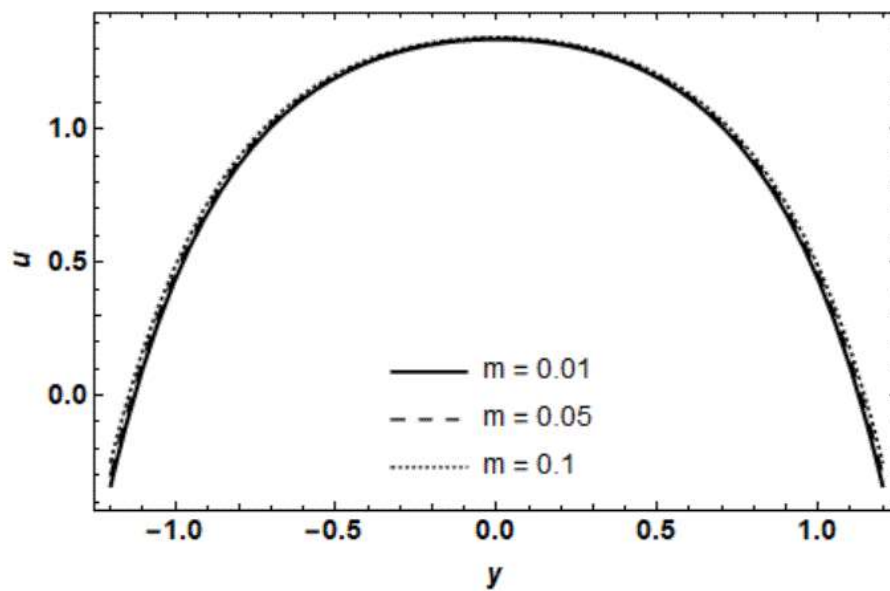
Figure 4.13 Effect of non-uniform parameter on velocity field.
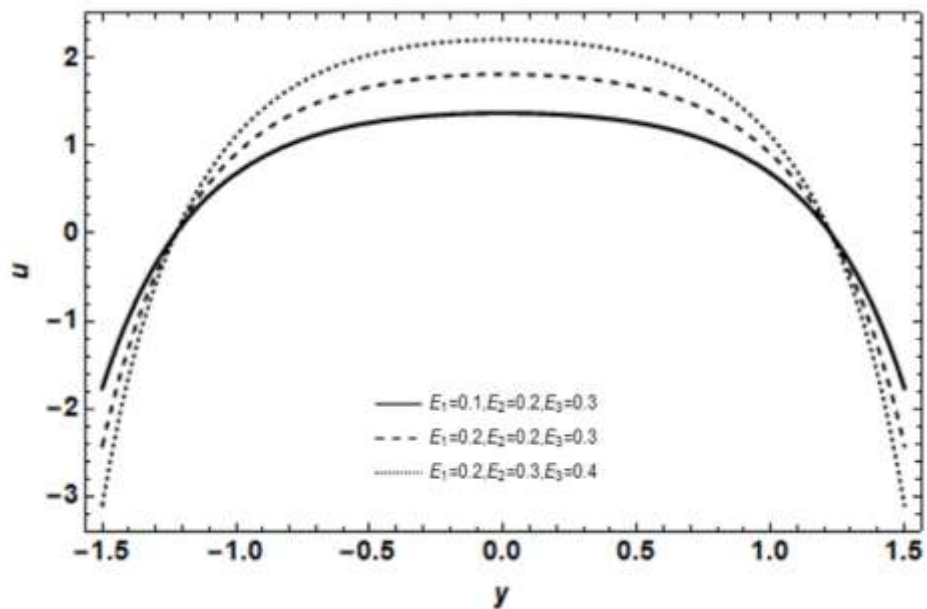
Figure 4.14 Effect of wall properties on velocity field.
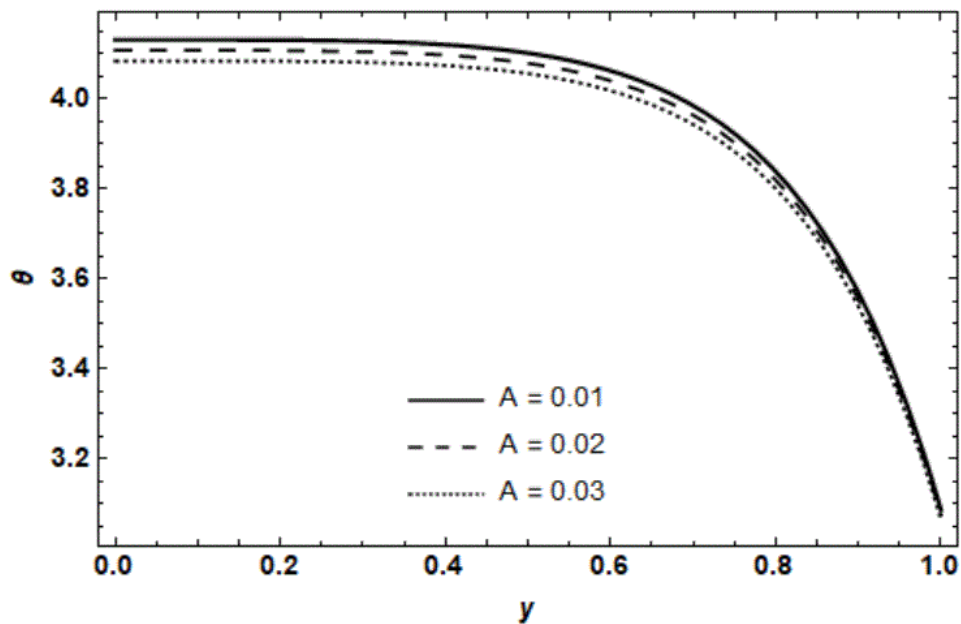
Figure 4.15 Effect of Eyring-Powell fluid parameter *A* on temperature profile.
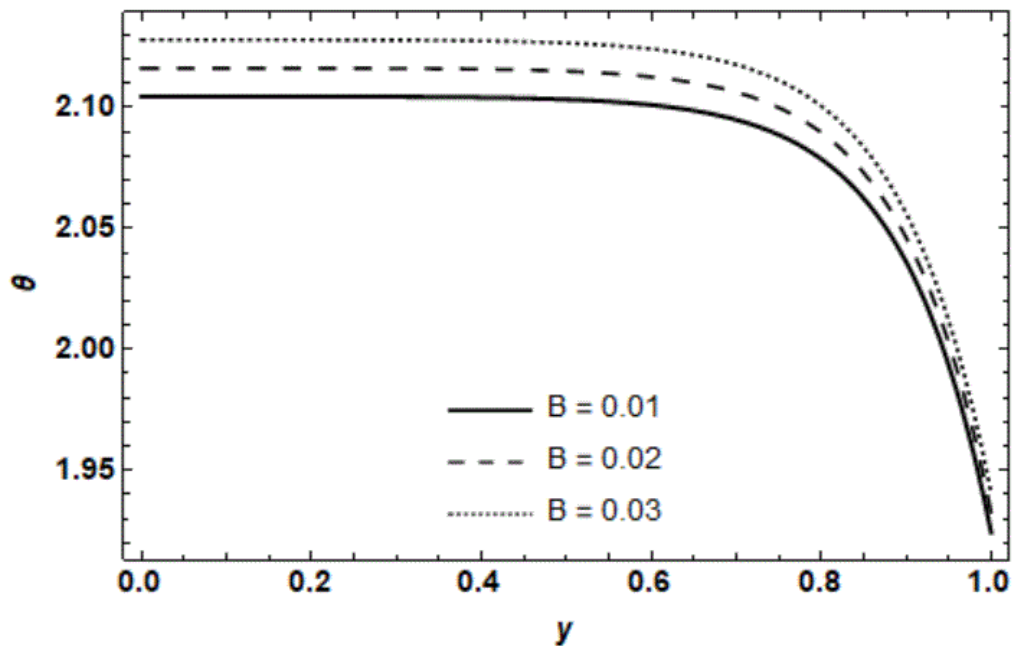
Figure 4.16 Effect of Eyring-Powell fluid parameter *B* on temperature field.

Figure 4.17 Effect of magnetic parameter on temperature field.

Figure 4.18 Effect of inclined parameter on temperature field

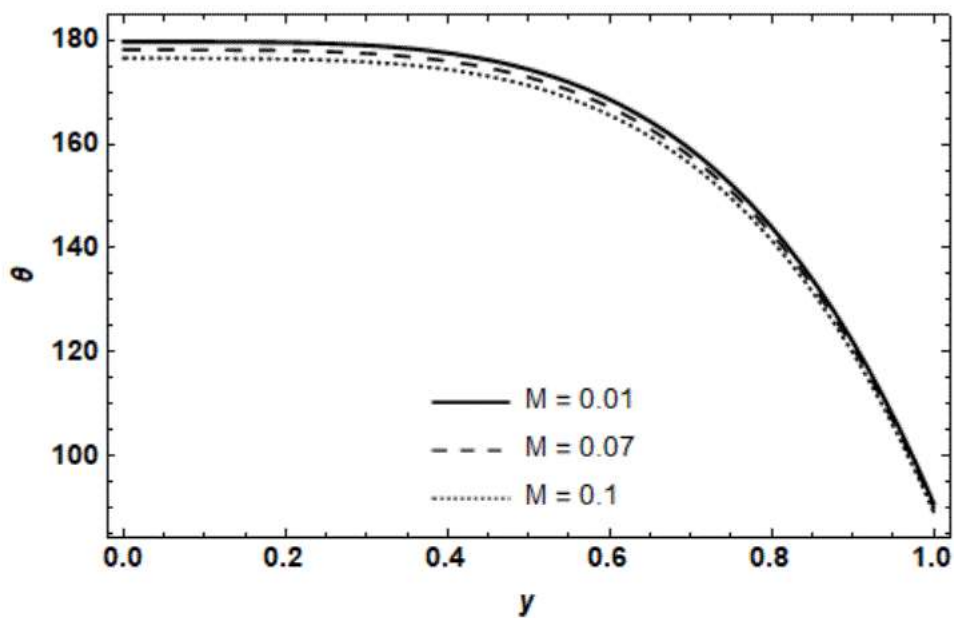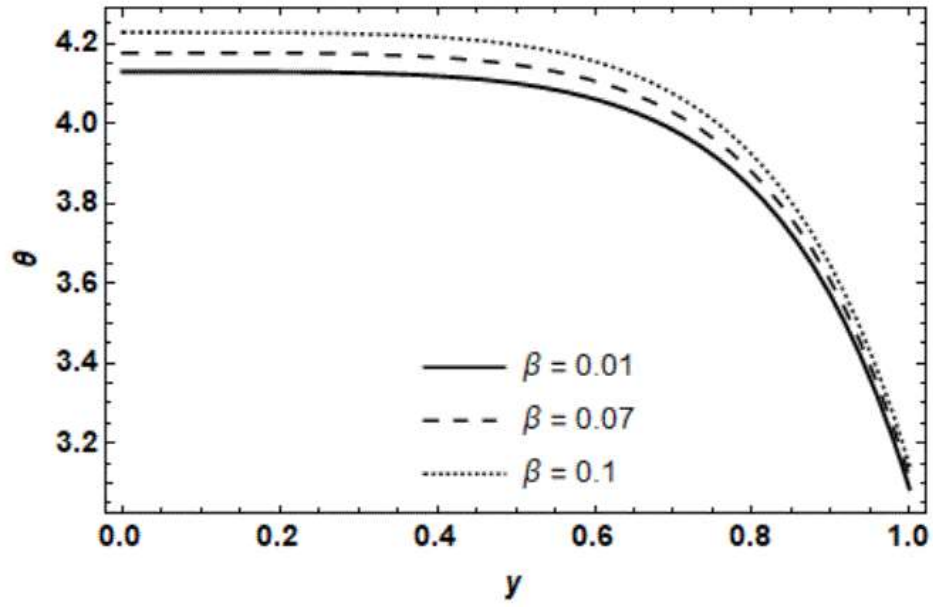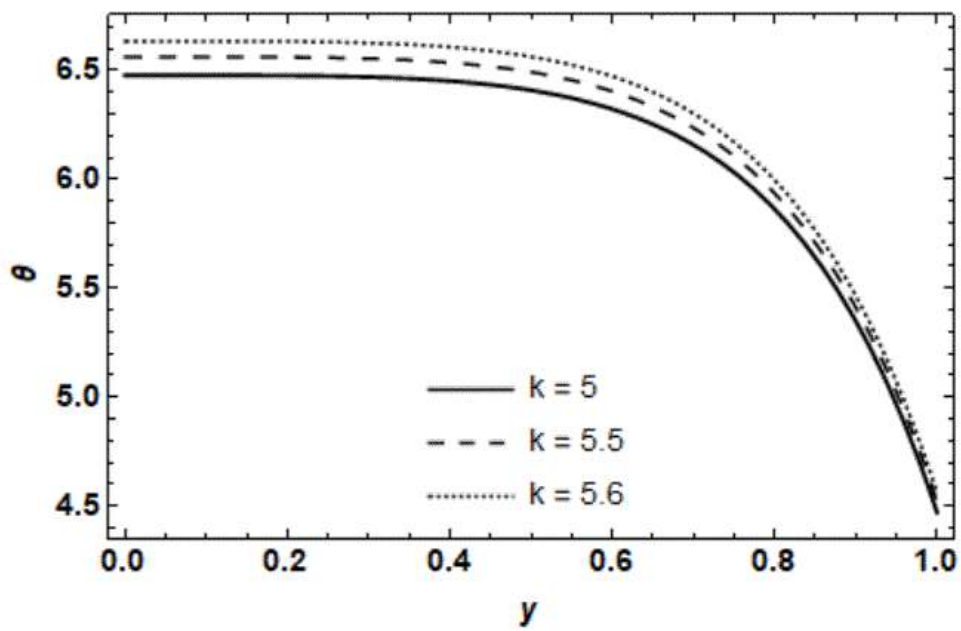**Figure 4.19** Effect of porosity parameter on temperature field.
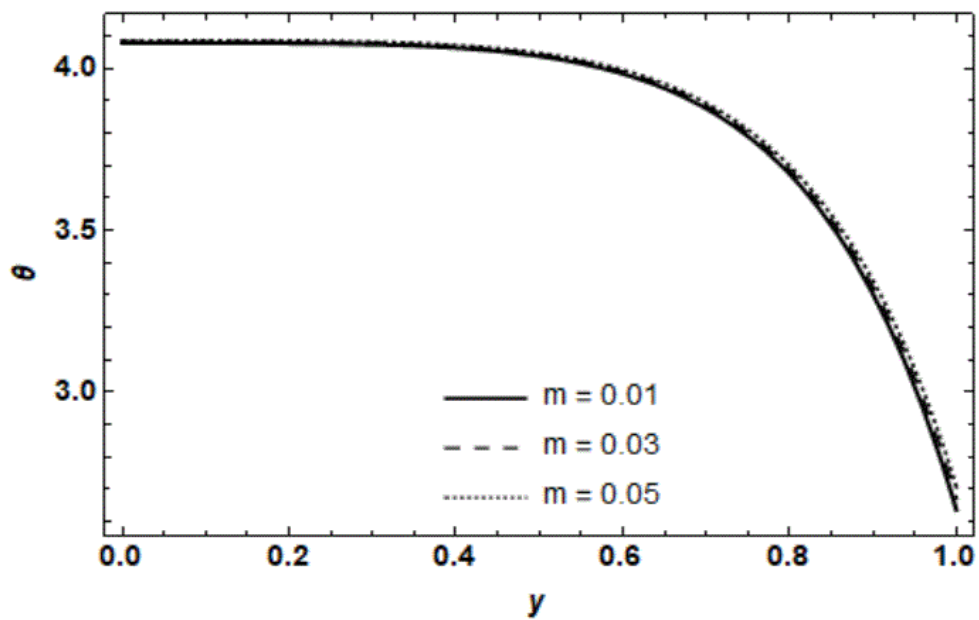
Figure 4.20 Effect of non-uniform parameter on temperature field.
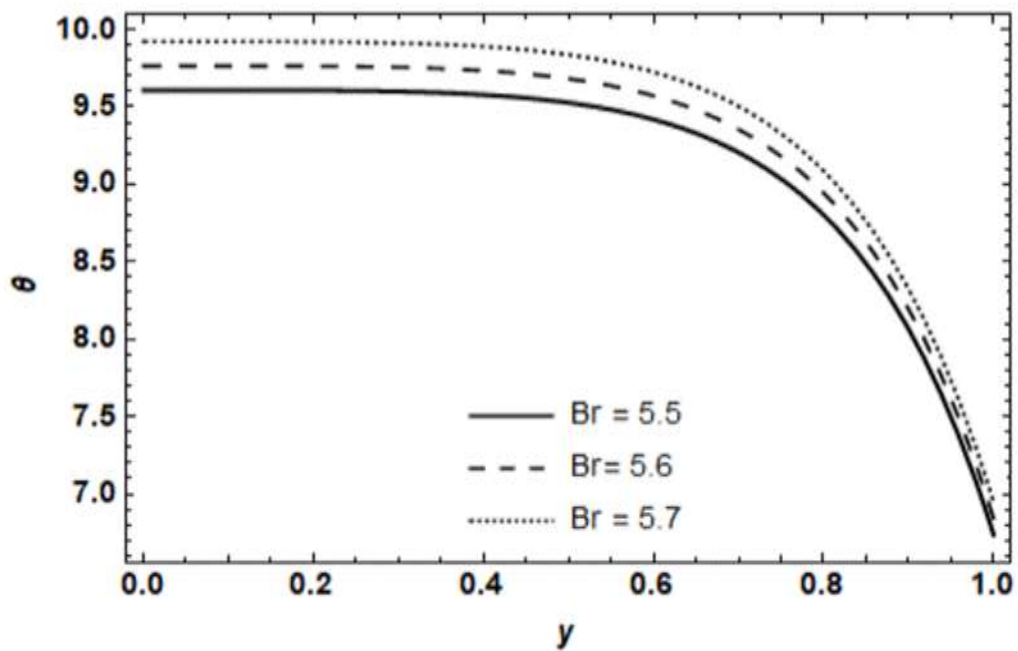
Figure 4.21 Effect of Brinkman Number on temperature field.
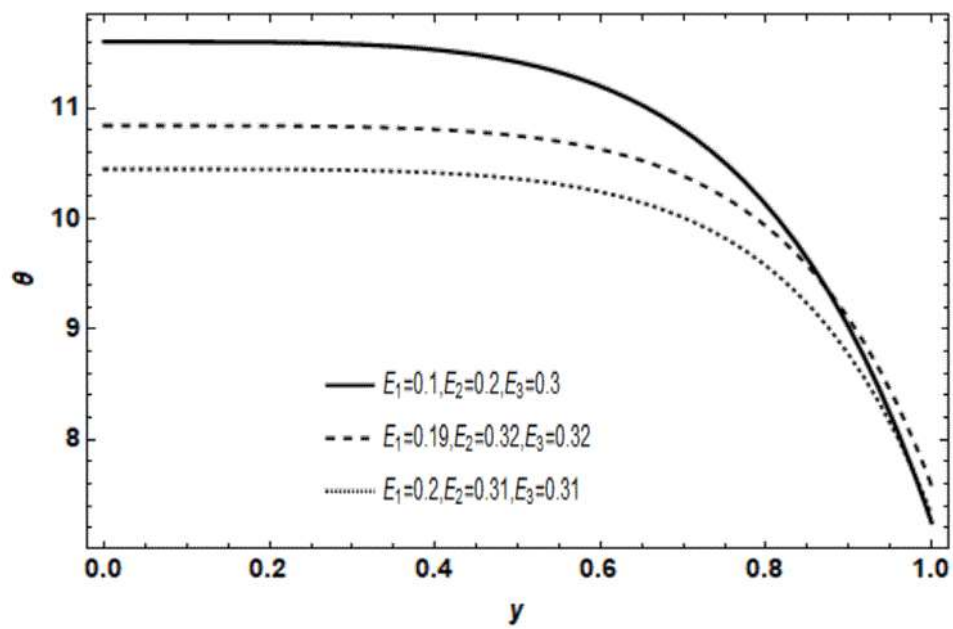
Figure 4.22 Effect of wall properties on temperature field.

CHAPTER 5

CONCLUSION AND FUTURE WORK

5.1 Conclusion

The purpose of this thesis is to investigate how porosity and an angled magnetic field affect the peristaltic flow of Eyring-Powell fluid. The complexity of problem can be addressed by using perturbation techniques, by using the lubrication approach. Graphical representation of velocity, stream function and temperature distribution are generated by using Mathematica software, providing visual insights into the behavior of peristaltic flow under different conditions. The overall conclusion drawn from the current work is summarized as following:

It is observed that by enhancing the value of parameters A, B and magnetic parameter M, the velocity of fluids decreases. While an increase in value of inclination angle β, porosity of wall, value of m, wall properties such as elasticity, damping parameter, accelerate the flow in an axial direction based on mass per unit area. As the magnetic parameter and Eyring-Powell fluid parameter A increase, the temperature profile falls. However, as the temperature rises, so do the larger values of the Brinkman number (Br), inclination angle β, porosity parameter k, and Eyring-Powell fluid parameter B.

The Eyring-Powell fluid parameter A and magnetic parameter influences the trapping effect, with higher values leading to a large bolus, while increasing B and value of inclination angle, size of bolus and number of streamlines decreases.

5.2 Future Work

The model could be expanded by adding additional factors such as energy activation and viscous dissipation. This could involve exploring different fluid models like Williamson and Walter's B fluid models as well as other non-Newtonian fluid models, to analyze the influence of inclined magnetic field and boundary slip. As our current study focused on non-uniform inclined channel, furture research could explore alternative geometries such as curved or planar channels. Additionally, incorporating boundary conditions such as slip and convective boundary conditions could provide furture insights into the behavior of peristaltic flow in practical scenarios.

REFERENCES

[1] Latham TW "Fluid motions in a peristaltic pump", Massachusetts Institute of Technology, Cambridge, 1966.

[2] A. H. Shapiro, M. Y. Jaffrin, and S. L. Weinberg, "Peristaltic pumping with long wavelengths at low Reynolds number," 1969.

[3] P. Nagarani, "Peristaltic transport of a casson fluid in an inclined channel," *Korea Aust. Rheol. J.*, vol. 22, no. 2, pp. 105–111, 2010.

[4] Burns J, Parkes T "Peristaltic motion", J Fluid Mech 29(4):731–743, 1967.

[5] M. M. Bhatti, M. A. Abbas, and M. M. Rashidi, "Combine effects of Magnetohydrodynamics (MHD) and partial slip on peristaltic Blood flow of Ree–Eyring fluid with wall properties," *Eng. Sci. Technol. an Int. J.*, vol. 19, no. 3, pp. 1497–1502, Sep. 2016, doi: 10.1016/j.jestch.2016.05.004.

[6] G. Sucharitha, K. Vajravelu, S. Sreenadh, and P. Lakshminarayana, "Peristaltic flow and heat transfer of a Herschel-Bulkley fluid in an inclined non-uniform channel with wall properties," in *IOP Conference Series: Materials Science and Engineering*, Institute of Physics Publishing, Dec. 2017. doi: 10.1088/1757-899X/263/6/062026.

[7] C. Rajashekhar, G. Manjunatha, K. V. Prasad, B. B. Divya, and H. Vaidya, "Peristaltic transport of two-layered blood flow using Herschel–Bulkley Model," *Cogent Eng.*, vol. 5, no. 1, pp. 1–16, Jan. 2018, doi: 10.1080/23311916.2018.1495592.

[8] H. M. Mansour and M. Y. Abou-Zeid, "Heat and Mass Transfer Effect on Non-Newtonian Fluid Flow in a Non-uniform Vertical Tube with Peristalsis," *J. Adv. Res. Fluid Mech. Therm. Sci. J. homepage*, vol. 61, pp. 44–62, 2019.

[9] D. Baliga, M. Gudekote, R. Choudhari, H. Vaidya, and K. V. Prasad, "Influence of Velocity and Thermal Slip on the Peristaltic Transport of a Herschel-Bulkley Fluid Through an Inclined Porous Tube," *J. Adv. Res. Fluid Mech. Therm. Sci. J. homepage*, vol. 56, pp. 195–210, 2019.

[10] S. M Puranik *et al.*, "Effect of heat transfer on peristaltic flow of Newtonian fluid through eccentric cylinders," *Case Stud. Therm. Eng.*, vol. 45, May 2023, doi: 10.1016/j.csite.2023.102912.

[11] N. S. Akbar and S. Nadeem, "Characteristics of heating scheme and mass transfer on the peristaltic flow for an Eyring-Powell fluid in an endoscope," *Int. J. Heat Mass Transf.*, vol. 55, no. 1–3, pp. 375–383, Jan. 2012, doi: 10.1016/j.ijheatmasstransfer.2011.09.029.

[12] S. Noreen and M. Qasim, "Peristaltic flow of MHD Eyring-Powell fluid in a channel," *Eur. Phys. J. Plus*, vol. 128, no. 8, Aug. 2013, doi: 10.1140/epjp/i2013-13091-3.

[13] A. A. Khan, F. Zaib, and A. Zaman, "Effects of entropy generation on Powell Eyring fluid in a porous channel," *J. Brazilian Soc. Mech. Sci. Eng.*, vol. 39, no. 12, pp. 5027–5036, Dec. 2017, doi: 10.1007/s40430-017-0881-y.

[14] B. Ahmed, T. Hayat, K. Muhammad, and A. Alsaedi, "MHD peristaltic activity of Powell-Eyring nanomaterial through porous space with slip effects," *Case Stud. Therm. Eng.*, vol. 45, May 2023, doi: 10.1016/j.csite.2023.103001.

[15] J. Iqbal, F. M. Abbasi, M. Alkinidri, and H. Alahmadi, "Heat and mass transfer analysis for MHD bioconvection peristaltic motion of Powell-Eyring nanofluid with variable thermal characteristics," *Case Stud. Therm. Eng.*, vol. 43, Mar. 2023, doi: 10.1016/j.csite.2022.102692.

[16] A. Bhattacharyya, R. Kumar, S. Bahadur, G. S. Seth, and Sunil, "Modeling and interpretation of peristaltic transport of Eyring–Powell fluid through uniform/non-uniform channel with Joule heating and wall flexibility," *Chinese J. Phys.*, vol. 80, no. December, pp. 167–182, 2022, doi: 10.1016/j.cjph.2022.06.018.

[17] M. Gudekote *et al.*, "Heat and mass transfer effects on peristaltic transport of eyring powell fluid through an inclined non-uniform channel," *Eng. Lett.*, vol. 31, no. 2, pp. 833–847, 2023.

[18] Y. Akbar, S. Huang, M. U. Ashraf, K. S. Nisar, and M. M. Alam, "Electrothermal analysis for reactive Powell Eyring nanofluid flow regulated by peristaltic pumping with mass transfer," *Case Stud. Therm. Eng.*, vol. 44, no. February, p. 102828, 2023, doi: 10.1016/j.csite.2023.102828.

[19] S. Nadeem, A. Mushtaq, J. Alzabut, H. A. Ghazwani, and S. M. Eldin, "The flow of an Eyring Powell Nanofluid in a porous peristaltic channel through a porous medium," *Sci. Rep.*, vol. 13, no. 1, pp. 1–16, 2023, doi: 10.1038/s41598-023-36136-x.

[20]   M. Boujelbene *et al.*, "Impact of variable slip and wall properties on peristaltic flow of eyring-powell fluid through inclined channel: artificial intelligence based perturbation technique," *Fractals*, vol. 31, no. 6, pp. 1–18, 2023, doi: 10.1142/S0218348X23401400.

[21]   S. Akram, M. Athar, K. Saeed, and A. Razia, "Theoretical analysis of partial slip on double-diffusion convection of Eyring-Powell nanofluids under the effects of peristaltic propulsion and inclined magnetic field," *J. Magn. Magn. Mater.*, vol. 569, no. January, p. 170445, 2023, doi: 10.1016/j.jmmm.2023.170445.

[22]   R. Choudhari *et al.*, "Analysis of peristalsis blood flow mechanism using non-newtonian fluid and variable liquid characteristics," *Results Eng.*, vol. 21, no. October 2023, p. 101842, 2024, doi: 10.1016/j.rineng.2024.101842.

[23]   Akbar, Yasir, Shiping Huang, Muhammad Usman Ashraf, Kottakkaran Sooppy Nisar, and Mohammad Mahtab Alam. "Electrothermal analysis for reactive Powell Eyring nanofluid flow regulated by peristaltic pumping with mass transfer." *Case Studies in Thermal Engineering* 44 (2023): 102828.

[24]   Whitaker, Stephen. "Flow in porous media I: A theoretical derivation of Darcy's law." *Transport in porous media* 1 (1986): 3-25.

[25]   F. H. Oyelami and M. S. Dada, "Unsteady magnetohydrodynamic flow of some non-Newtonian fluids with slip through porous channel," *Int. J. Heat Technol.*, vol. 36, no. 2, pp. 709–713, 2018, doi: 10.18280/ijht.360237.

[26]   M. Nazeer, A. Al-Zubaidi, F. Hussain, F. Z. Duraihem, S. Anila, and S. Saleem, "Thermal transport of two-phase physiological flow of non-Newtonian fluid through an inclined channel with flexible walls," *Case Stud. Therm. Eng.*, vol. 35, Jul. 2022, doi: 10.1016/j.csite.2022.102146.

[27]   I. M. Eldesoky, M. S. Nayel, A. A. Galal, and H. M. Raslan, "Combined effects of space porosity and wall properties on a compressible maxwell fluid with MHD peristalsis," *SN Appl. Sci.*, vol. 2, no. 12, pp. 1–14, 2020, doi: 10.1007/s42452-020-03878-6.

[28]   K. Javid, Z. Asghar, U. Saeed, and M. Waqas, "Porosity effects on the peristaltic flow of biological fluid in a complex wavy channel," *Pramana - J. Phys.*, vol. 96, no. 1, 2022, doi: 10.1007/s12043-021-02241-7.

[29]   S. Noreen, T. Kausar, D. Tripathi, Q. U. Ain, and D. C. Lu, "Heat transfer analysis on creeping flow Carreau fluid driven by peristaltic pumping in an inclined asymmetric channel," *Therm. Sci. Eng. Prog.*, vol. 17, no. January, 2020, doi: 10.1016/j.tsep.2020.100486.

[30] B. Ahmed, D. Liu, Y. Zhang, and M. A. Hussien, "Peristaltic pumping of convective nanofluid with magnetic field and thermal radiation in a porous channel," *Case Stud. Therm. Eng.*, vol. 53, no. October 2023, p. 103918, 2024, doi: 10.1016/j.csite.2023.103918.

[31] Vijayaragavan, R., P. Tamizharasi, and A. Magesh. "Peristaltic motion of Non-Newtonian fluid under the influence of inclined magnetic field, porous medium and chemical reaction." Scientia Iranica (2024).

[32] Jagadesh, V., S. Sreenadh, M. Ajithkumar, P. Lakshminarayana, and G. Sucharitha. "Investigation of dissipative heat transfer and peristaltic pumping on MHD Casson fluid flow in an inclined channel filled with porous medium." Numerical Heat Transfer, Part B: Fundamentals (2023): 1-19.

[33] M. Devakar, K. Ramesh, and K. Vajravelu, "Magnetohydrodynamic effects on the peristaltic flow of couple stress fluid in an inclined tube with endoscope," *J. Comput. Math. Data Sci.*, vol. 2, p. 100025, Jan. 2022, doi: 10.1016/j.jcmds.2022.100025.

[34] A. A. Khan and R. Rafaqat, "Effects of radiation and MHD on compressible Jeffrey fluid with peristalsis," *J. Therm. Anal. Calorim.*, vol. 143, no. 3, pp. 2775–2787, 2021, doi: 10.1007/s10973-020-10045-x.

[35] N. T. M. El-Dabe, M. Y. Abou-Zeid, M. A. A. Mohamed, and M. M. Abd-Elmoneim, "MHD peristaltic flow of non-Newtonian power-law nanofluid through a non-Darcy porous medium inside a non-uniform inclined channel," *Arch. Appl. Mech.*, vol. 91, no. 3, pp. 1067–1077, 2021, doi: 10.1007/s00419-020-01810-3.

[36] M. Rafiq, A. Shaheen, Y. Trabelsi, S. M. Eldin, M. I. Khan, and D. K. Suker, "Impact of activation energy and variable properties on peristaltic flow through porous wall channel," *Sci. Rep.*, vol. 13, no. 1, pp. 1–19, 2023, doi: 10.1038/s41598-023-30334-3.

[37] A. M. Abd-Alla, E. N. Thabet, and F. S. Bayones, "Numerical solution for MHD peristaltic transport in an inclined nanofluid symmetric channel with porous medium," *Sci. Rep.*, vol. 12, no. 1, pp. 1–11, 2022, doi: 10.1038/s41598-022-07193-5.

[38] T. Hayat, W. Rehman, B. Ahmed, and S. Momani, "Peristalsis for MHD hybrid nanomaterial through asymmetric channel," *Alexandria Eng. J.*, vol. 78, no. March, pp. 65–73, 2023, doi: 10.1016/j.aej.2023.07.014.

[39] N. M. Hafez, A. M. Abd-Alla, and T. M. N. Metwaly, "Influences of rotation and mass and heat transfer on MHD peristaltic transport of Casson fluid through inclined plane," *Alexandria Eng. J.*, vol. 68, pp. 665–692, 2023, doi: 10.1016/j.aej.2023.01.038.

[40] A. Tanveer, M. B. Ashraf, and M. Masood, "Entropy analysis of peristaltic flow over curved channel under the impact of MHD and convective conditions," *Numer. Heat Transf. Part B Fundam.*, vol. 85, no. 1, pp. 45–57, 2024, doi: 10.1080/10407790.2023.2224507.

[41] S. A. Hussein and N. T. Eldabe, "Peristaltic transport of radiative and dissipative MHD third order nanofluid through the vertical asymmetric channel with heat and mass convection," *Int. J. Ambient Energy*, vol. 45, no. 1, 2024, doi: 10.1080/01430750.2023.2266435.

[42] J. Iqbal and F. M. Abbasi, "Peristaltic transport of hybrid nanofluid under the effects of thermal radiation through asymmetric curved geometry: a numerical approach," *Int. J. Model. Simul.*, vol. 00, no. 00, pp. 1–18, 2024, doi: 10.1080/02286203.2023.2296614.

[43] A. Magesh, P. Praveen Kumar, P. Tamizharasi, R. Vijayaragavan, S. Vimal Kumar, and M. Kothandapani, "Effect of magnetic field on the peristaltic transport of Oldroyd-B fluid in an asymmetric inclined channel," *J. Phys. Conf. Ser.*, vol. 1850, no. 1, 2021, doi: 10.1088/1742-6596/1850/1/012111.

[44] A. Tanveer and S. Jarral, "Inclined MHD Effects in Tapered Asymmetric Porous Channel with Peristalsis: Applications in Biomedicine," *Sci. Eng. Technol.*, vol. 3, no. 2, pp. 36–46, 2023, doi: 10.54327/set2023/v3.i2.68.

[45] Y. Elmhedy, A. M. Abd-Alla, S. M. Abo-Dahab, F. M. Alharbi, and M. A. Abdelhafez, "Influence of inclined magnetic field and heat transfer on the peristaltic flow of Rabinowitsch fluid model in an inclined channel," *Sci. Rep.*, vol. 14, no. 1, pp. 1–15, 2024, doi: 10.1038/s41598-024-54396-z.

[46] S. Akram, M. Athar, and K. Saeed, "Hybrid impact of thermal and concentration convection on peristaltic pumping of Prandtl nanofluids in non-uniform inclined channel and magnetic field," *Case Stud. Therm. Eng.*, vol. 25, Jun. 2021, doi: 10.1016/j.csite.2021.100965.

[47] R. Shukla, S. S. Bhatt, A. Medhavi, R. Kumar, and C. Llopis-Albert, "Effect of Surface Roughness during Peristaltic Movement in a Nonuniform Channel," *Math. Probl. Eng.*, vol. 2020, 2020, doi: 10.1155/2020/9643425.

[48] C. Rajashekhar, H. Vaidya, K. V. Prasad, I. Tlili, A. Patil, and P. Nagathan, "Unsteady flow of Rabinowitsch fluid peristaltic transport in a non-uniform channel with temperature-dependent properties," *Alexandria Eng. J.*, vol. 59, no. 6, pp. 4745–4758, 2020, doi: 10.1016/j.aej.2020.08.036.

[49] Y. Khan, S. Akram, A. Razia, A. Hussain, and H. A. Alsulaimani, "Effects of Double Diffusive Convection and Inclined Magnetic Field on the Peristaltic Flow of Fourth Grade

Nanofluids in a Non-Uniform Channel," *Nanomaterials*, vol. 12, no. 17, 2022, doi: 10.3390/nano12173037.

[50] M. G. Ibrahim and M. Y. Abou-zeid, "Influence of variable velocity slip condition and activation energy on MHD peristaltic flow of Prandtl nanofluid through a non-uniform channel," *Sci. Rep.*, vol. 12, no. 1, pp. 1–12, 2022, doi: 10.1038/s41598-022-23308-4.

[51] G. Manjunatha, C. Rajashekhar, H. Vaidya, K. V. Prasad, and K. Vajravelu, "Impact of heat and mass transfer on the peristaltic mechanism of Jeffery fluid in a non-uniform porous channel with variable viscosity and thermal conductivity," *J. Therm. Anal. Calorim.*, vol. 139, no. 2, pp. 1213–1228, 2020, doi: 10.1007/s10973-019-08527-8.

[52] Smith, Roger K. "Introductory lectures on fluid dynamics." Monash University, Australia (2008).

[53] Dr. R.K. Bansal, "Fluid Mechanics & Hydraulic Machines," *Laxmi Publications*. pp. 163–165, 2005.

[54] Pritchard, Philip J., and John W. Mitchell. Fox and McDonald's introduction to fluid mechanics. John Wiley Sons, 2016.

[55] Hina, S. "MHD peristaltic transport of Eyring–Powell fluid with heat/mass transfer, wall properties and slip conditions." *Journal of Magnetism and Magnetic Materials* 404 (2016): 148-158.